THE UNIVERSITY OF READING

Crowded – Macroscopic and Microscopic Models for Pedestrian Dynamics

Penny Marno

Numerical Analysis Report 4/2002

DEPARTMENT OF MATHEMATICS

Crowded - Macroscopic and Microscopic Models for Pedestrian Dynamics

Penny Marno

September 1st 2002

Abstract

Pedestrian models have been studied for about 40 years. Initially focusing on macroscopic models which consider a crowd as a fluid or granular flow, more recent research has developed microscopic models of individual pedestrian behaviour in crowds. These include terms to model human psychology such as the desire to keep a certain distance from other people. This dissertation uses a transformation developed within a traffic context to move from a microscopic to a macroscopic model whilst retaining some of the psychological factors. Primarily in a 1-dimensional framework, Lax-Friedrichs, Upwind and Lax-Wendroff numerical schemes are used to solve the resulting system of hyperbolic equations numerically. Some work is also undertaken on a 2-dimensional model, developing an analogous transformation which is used to derive a more sophisticated model of pedestrian behaviour. This is solved using dimensional splitting techniques.

Declaration

I confirm that this is my own work and the use of all materials from other sources has been properly and fully acknowledged.

Signed 

Acknowledgements

I would like to thank my supervisors Professor Mike Baines and Dr Peter Sweby for their help with, and enthusiasm for this project. Their approachability, patience and inspiration has been superb. I am also very grateful to Sue Davis for her assistance, and to my fellow MSc students for their friendship and encouragement.

Many thanks also go to the EPSRC for their generous financial support throughout this course.

Finally I would like to thank Rob and my family for their love and support.

Contents

List of Figures

Chapter 1

Introduction

Pedestrian crowd modelling has been studied for over 40 years. The models are particularly used for evacuation and disaster scenario modelling, but can be a key part of any building development or emergency planning procedures.

The main models used here are those developed by Dirk Helbing [6] - [9] but there are a range of other approaches which will be reviewed briefly. The subject area cuts across mathematics, psychology and computer science and many of the approaches developed focus on their use as a practical tool to non-mathematicians: their benchmark is purely to mirror observational data. However as many of the models are analogous to those developed for traffic modelling, they can be solved numerically as systems of hyperbolic equations in conservation law form

$$\frac{\partial \underline{u}}{\partial t} + \frac{\partial \underline{f}(u)}{\partial x} = \underline{s}(u) \tag{1.1}$$

where $\underline{u}$ is the conserved quantity, $\underline{f}(u)$ is the flux and $\underline{s}(u)$ is a source term.

There are two main types of model: macroscopic models which model crowd behaviour as an entity in itself and draw from gas and fluid flow approaches, and microscopic models which consider each pedestrian and his or her individual preferences. The latter are considered to be advantageous as they are more sensitive and better reflect the effects of collision and interaction behaviour. However macroscopic

models can be more computationally efficient. A number of ways of moving from micro to macro models (and vice versa) have been developed, mainly for traffic models. This report will consider in detail the approach developed by Peter Berg and Anthony Woods [2] for traffic where a microscopic model is 'converted' into a system of conservation laws. These can then be solved using standard numerical techniques and their stability and behaviour investigated. If this approach works, it will provide a simpler macroscopic model than those previously developed whilst incorporating some of the strengths of the microscopic model.

Chapter 2 contains a brief literature review on pedestrian modelling, particularly focusing on microscopic and macroscopic models and the relationship between them. Helbing [9] has developed a social force model which takes into account some of the psychology of crowd interaction on a microscopic level. We define this model and explain the Berg and Woods approach for moving between a microscopic and macroscopic traffic model. Chapter 3 looks briefly at the numerical methods which can be used in solving hyperbolic equations and explains how to derive the truncation error and stability region for the schemes we shall use. One of the challenges of the model is the complexity of the source term and how this can be dealt with. In Chapter 4 we apply the approach to the model, looking at a one-dimensional case of people moving along a corridor. For some initial results we make various simplifying assumptions and then use some numerical schemes including Lax-Friedrichs and Upwinding to look at solutions and their stability. Both initial and boundary conditions are varied in order to see how this affects the results and whether they have a physical interpretation. In Chapter 5 we extend the model further to consider a two-dimensional situation, where people are able to overtake each other and, for example, move towards a doorway or specified exit. Finally Chapter 6 will outline the conclusions which can be drawn from both the approach and the results.

Chapter 2

Pedestrian Modelling Research

2.1 Introduction

Pedestrian or crowd modelling has been of interest to the scientific community for many years. Initially, models were developed from observational data, and photographs and videotapes studied to assess the movement and behaviour of people in crowd situations. It was noticed that crowds reflected the flow of fluids or granules in certain cases and this inspired people to model crowds using equations based on physical phenomena. Many of these models used some sort of conservation equation but over time it was shown that these fluid or granular based models did not capture enough of the psychological behaviour of humans. For example, molecules do not keep their distance from other molecules they do not like, or get distracted by interesting events at the boundary, whereas people generally prefer to maintain some personal space between themselves and others and may be attracted to, for example, an attractive shop window display in a pedestrian street. Modelling whole crowd behaviour rather than individual preferences results in what are known as macroscopic models, whereas those which simulate individual pedestrian behaviour are called microscopic.

Research covers modelling both normal pedestrian behaviour, and evacuation and

panic activity. The latter is more complicated as people generally cease to behave in a rational manner, and exhibit herd like behaviour [19], following each other rather than thinking a course of action through, which can lead to overcrowding and injury. People catching others up and bunching can, mathematically, produce waves and shocks.

There are clearly parallels between traffic and pedestrian modelling both in the nature of the modelling and psychology of behaviour of pedestrians and drivers, and in the divide between macroscopic and microscopic models. Macroscopic traffic models are often used as they give insight into throughput, density distributions and the onset of jams. Lighthill and Witham [18] developed probably the most famous. The macroscopic /microscopic analogy for traffic models is the continuum model where traffic flow is modelled on an open road and individual vehicles are smoothed out into continuous velocity and density fields (macroscopic), and the car following approach where the behaviour of each vehicle is linked to that of the vehicle in front by a mathematical rule (microscopic).

For microscopic or car following approaches, individual psychologies can be incorporated and these models can distinguish between the behaviour of, for example, trucks and cars, slow and fast moving cars or vehicles in different weather conditions [14]. The microscopic to macroscopic conversion by Berg and Woods [2] which is used here has been developed specifically for a traffic model but we adapt it for crowd flow.

We will now consider some of the main macro and micro models in more detail.

2.2 Macroscopic Models

These treat the dynamics of the crowd as one body, often in a similar way to a fluid or gas flow, although others have been developed using queuing theory, transition matrices or route choice behaviour models.

In 1971, Henderson [16] developed a statistical model of crowd flow and showed

that a loosely packed crowd would flow like a gas whilst a densely packed crowd was more similar to liquid flow. His model used Maxwell Boltzmann Theory to define a probability density function of velocity:

$$P(V_x') \equiv \frac{1}{\sqrt{2\pi}v_{\text{r.m.s.}}} exp\Big(-\frac{1}{2}\frac{V_x'^2}{v_{\text{r.m.s.}}^2}\Big) \tag{2.1}$$

where

V_x = component of the mean velocity of the flux

$v_{r.m.s.}$ = root mean square of the speed v.

He compared his results to observational data and found it matched the behaviour of certain groups such as students. However it struggles near maximum values and further research showed that behaviour changes depending on the gender balance of the crowd. The microscopic model incorporating preferences has much more scope for modelling this.

In 1999, Helbing and Viscek [8] developed a continuum model looking at the interactions between two sub-populations. In this a and b are two sub populations with different desired walking directions and the equation for a population a is given by:

$$\frac{\partial \rho_a(x,t)}{\partial t} + \frac{\partial}{\partial x}[\rho_a(x,t)V_a(x,t)] = 0 \tag{2.2}$$

where

$\rho_a(x,t)$ = density

$V_a(x,t)$ = average velocity of pedestrians of population a perpendicular to their desired walking direction.

$V_a(x,t)$ is proportional to the frequency of interactions that a pedestrian of population a encounters with other pedestrians and the average amount $\triangle x$ that a pedestrian moves aside when evading another pedestrian, giving an expression of the form

$$V_a(x,t) \approx -c(\triangle x)^2\Big(C_{aa}\frac{\partial \rho_a}{\partial x} + C_{ab}\frac{\partial \rho_b}{\partial x}\Big)$$

where

c = prefactor allowing for slowing down in crowded areas

$C_{ab} > C_{aa}$ relates to the spatial areas used. This is developed in terms of a parameter measuring the effects of 'crowdedness', and the conditions for self-organisation. This adds a diffusion term to the above equation and its stability can be investigated.

Helbing [7] also developed a fluid dynamic model based on a Boltzmann-like gas kinetic model, with equivalent expressions modelling pressure and temperature, resulting in equations for mass density, momentum density and energy density. However the equations are somewhat complex although they do give reasonable results.

The primary difficulty with macroscopic models is that they do not allow for individual behaviour, e.g. deceleration or avoidance by people. As explained earlier, although at high densities there is evidence to suggest that crowds act like fluid or granular flow, macroscopic models do not take into account the self-organisation effects of people or their manoeuvrability. In panic situations [19], it can be shown that people tend not to take the most rational course of action. For example, people tend to follow the crowd and will follow each other and bunch around an already blocked exit in a smoke filled room regardless of other exits which may be available: a flow model would show people moving equally to all exits.

2.3 Microscopic Models

Behavioural models can be used as a basis for a range of situations where responses depend on individual preferences. A good review of work in this area is provided by Helbing, Farkas, Molnar and Viscek [6]. Current research is focused on microcopic simulation and the main approaches are:

- behavioural/social force models
- cellular automata models

- Artificial Intelligence - based models

We shall not consider the latter but references for them are given in [6].

The effectiveness of a microscopic model, like the behaviour force one, depends on its ability to reflect the preferences and behaviours of each person. Helbing *et al* [6] have studied observational data in detail and concluded that people:

- tend to choose the fastest not the shortest route, although they are not keen to take detours even if the way ahead is crowded
- have a preferred individual desired walking speed which is generally the most comfortable (i.e. least energy consuming) unless they need to be somewhere by a certain time. Within pedestrian crowds, these speeds are normally distributed with mean 1.34m/s and standard deviation 0.26m/s [16]. These figures are used in our model.
- keep a certain distance to other pedestrians and borders, depending on the extent to which a person is in a hurry and the density.
- get nervous in panic situations, move faster than normal, bump into others and exhibit herd behaviour
- show oscillatory behaviour at bottlenecks and the appearance of shocks in dense pedestrian crowds pushing forward.
- become obstacles if injured in panic situations, overlook alternative exits and can build up pressure to dangerous levels.

The behavioural force model reflects most of these behaviours.

2.3.1 Behavioural Force Model

This is one of the main microscopic models and has been developed from social field approaches in social psychology which allow for different behaviours [9]. These

assume that behaviour in conflict situations can be described by the addition of forces reflecting different environment influences. The approach has been applied to opinion formation, migration and traffic modelling as well as pedestrians. Although the model describes the interaction of specific individuals, Helbing [6] also comments that reliable crowd models can come from knowing the proportion of people exhibiting certain characteristics and that *'In some sense, the uncertainty about the individual behaviours is averaged out at the macroscopic level of description'*. This is important for work in subsequent chapters.

The behaviour force model is:

$$\frac{dv_i(t)}{dt} = \underbrace{\frac{v_i^0(t)e_i^0(t)}{\tau_i}}_{\text{driving term}} + \underbrace{\frac{\xi_i(t) - v_i(t)}{\tau_i}}_{\text{friction term}} + f_{ij}^{soc}(t) + f_{ij}^{ph}(t) + f_{ij}^{b} \tag{2.3}$$

where

$$\begin{aligned}
i, j &= \text{two bodies} \\
v_i(t) &= \text{velocity of body } i \\
v_i^0(t) &= \text{desired speed} \\
e_i^0(t) &= \text{desired direction of motion} \\
\tau_i &= \text{relaxation time} \\
\xi_i(t) &= \text{fluctuations} \\
f_{ij}^{soc}(t) &= \text{forces associated with socio-psychological contribution} \\
f_{ij}^{ph}(t) &= \text{forces associated with physical interactions} \\
f_{ij}^{b} &= \text{forces associated with boundary interactions.}
\end{aligned}$$

The repulsive social force term $f_{ij}^{soc}(t)$ is the socio-psychological contribution, reflecting the tendency of pedestrians to keep a certain distance from other pedestrians and can be written as:

$$f_{ij}^{soc}(t) = A_i exp[\frac{(r_{ij} - d_{ij})}{B_i}]n_{ij}\Big(\lambda_i + (1 - \lambda_i)\frac{1 + \cos\psi_{ij}}{2}\Big) \tag{2.4}$$

where

$$
\begin{aligned}
A_i &= \text{interaction strength} \\
r_{ij} &= \text{radius } i + \text{radius } j \\
d_{ij}(t) &= \| x_i - x_j \| \text{ ,distance between centres of mass of pedestrians i and j} \\
B_i &= \text{range of repulsive interactions, can be culturally dependent} \\
n_{ij} &= \frac{x_i(t) - x_j(t)}{d_{ij}(t)} \text{ normalized vector pointing from j to i} \\
\lambda_i &= \text{allows for anisotropic characters of pedestrian interactions, } < 1 \\
\psi_{ij} &= \text{angle between } e_i(t) = \frac{v_i(t)}{\|v_i(t)\|} \text{ and direction } -n_{ij}(t) \text{ of the} \\
&\quad \text{object exerting the repulsive force.}
\end{aligned}
$$

A_i would take a value between 0 and 1. Measures for the radius of a person come from Fruin data (see [23] or[5]), for example

Type	Breadth(cm)	Depth(cm)	Area(m^2)
British male	51	32.5	0.26
British female	43.5	30.5	0.21
Average(European)	45.58	28.2	0.2
Maximum	51.5	32.5	0.26

$f_{ij}^{ph}(t)$ is the physical interaction term which only plays a part if pedestrians have physical contact with each other, for example in a panic situation:

$$
f_{ij}^{ph}(t) = \underbrace{k\Theta(r_{ij} - d_{ij})n_{ij}}_{\text{body force}} + \underbrace{\kappa\Theta(r_{ij} - d_{ij})\Delta v_{ji}^t t_{ij}}_{\text{sliding friction force}} \tag{2.5}
$$

where

$$
\begin{aligned}
k, \kappa &= \text{large constants} \\
\Theta(z) &= z \text{ if } z \geq 0, \text{ otherwise } 0
\end{aligned}
$$

$$\Delta v_{ji}^{t} = (v_j - v_i)t_{ij}.$$

There is also possible interaction with boundaries such as walls,

$$f_{ib} = \Big(A_i exp\frac{(r_i - d_{ib})}{B_i} + k\Theta(r_i - d_{ib})\Big)n_{ib} - \kappa\Theta(r_i - d_{ib})(v_i t_{ib})t_{ib} \qquad (2.6)$$

where

$$\begin{aligned} d_{ib} &= \text{distance to boundary b} \\ n_{ib} &= \text{direction perpendicular to boundary} \\ t_{ib} &= \text{direction tangential to boundary.} \end{aligned}$$

In addition terms can be added for time-dependent attractive interactions such as being drawn to window displays, or to reflect the joining behaviour of families, friends or tourist groups.

Simulation of the model shows

- pedestrians tend to organise themselves into lanes of people with the same desired direction, eventually self organizing themselves into an optimal state [8]
- oscillations at bottlenecks, assuming people do not panic where small groups of people take it in turns to past through an exit in different directions

In panic situations the nonlinearity of pedestrian interactions exhibits

- 'freezing by heating' (increased energy leads to increased order, jamming and freezing giving a metastable state. This can be modelled by $\eta_i = (1 - \eta_i^{'})\eta_0 + \eta_i^{'}\eta_{max}$ (where $0 \leq \eta_i^{'} \leq 1$ measures the nervousness of pedestrian i) [12])
- faster-is-slower effect, i.e. the faster people move the more they get in the way of others and cause bunching and blockages

- phantom panics where a delay at the front, perhaps due to the faster-is-slower effect, causes those behind who cannot see a reason for the delay to begin to push and cause panic

- herding behaviour where people cease to act as individuals and follow their neighbours. This can be modelled by considering the desired direction $e_i^0(t) = N((1 - n_i)e_i + n_i < e_j^0(t) >_i)$ where each pedestrian can follow an individual direction e_i or the average direction $< e_j^0(t) >$ of his neighbours j in a certain radius and his options are weighted with a 'nervousness' factor n_i. If n_i is high we get herding behaviour.

Helbing uses the behavioural force model to produce simulations illustrating behaviour at intersections and avoidance of others. This suggests that it can work in two dimensions although still based around the interactions of just two people. To move properly into two dimensions, we would need to look at the interactions between more than two people and introduce more sophisticated terms for position, radius, direction etc. Some of Helbing's results can be found on-line at *www.helbing.org* and are simulated through Java applets.

This model appears to be the most effective both in representing the psychological behaviour of individuals but also in capturing the behaviours of crowds which match observation data. In the following chapters we will use this model as a basis for developing a macroscopic model, attempting to reflect some of the behavioural results at the higher level with a more simple model than that seen in Section 2.2. Firstly we outline the conversion process from microscopic to macroscopic models developed by Berg and Woods.

2.4 Microscopic to Macroscopic Models

The transistion between microscopic and macroscopic models (and back again) has been explored by a number of people for traffic dynamics, in particular Helbing [13], Zhang [30] and the approach used here by Berg and Woods [2]. This section outlines the approach used by Berg and Woods for cars and in their paper they continue further to analyse the stability and behaviour of the resulting macroscopic model.

The density of cars ρ is usually described as simply the inverse of the headway b but this does not work when transferring from microscopic to macroscopic models so some other way of mapping $\{x_i\} \mapsto [\rho : \Re \to \Re]$ is needed, where x_i is the position of a vehicle at a given instant in time . Starting with the requirement $\int_{x_i}^{x_{i+1}} \rho(x,t)dx = 1$ for all i, we can use the definition of headway $b = x_{i+1} - x_i$ to extend this function to all points along the road to give

$$\int_{x}^{x+b(x,t)} \rho(x^{'},t)dx^{'} = \int_{0}^{b(x,t)} \rho(x+y,t)dy \equiv 1 \tag{2.7}$$

Here we are considering a region of road $(1, y)$ and hence the integral is with respect to its length. Taking a Taylor expansion of $\rho(x+y,t)$, integrating with respect to y and truncating after the second order we get

$$b\rho + \frac{1}{2!}b^2\rho_x + \frac{1}{3!}b^3\rho_{xx} = 1. \tag{2.8}$$

By assuming that each term is of smaller magnitude than the one preceding it, we can ignore the cubic terms and solving as a quadratic in b gives $b = \frac{1}{\rho} - \frac{\rho_x}{2\rho^3}$ and regarding the cubic term as a perturbation, expanding b gives a new expression in terms of ρ:

$$b \approx \underbrace{\frac{1}{\rho}}_{\text{usual relationship}} - \underbrace{\frac{\rho_x}{2\rho^3}}_{\text{pressure term}} - \underbrace{\frac{\rho_{xx}}{6\rho^4}}_{\text{dispersive term}} + \frac{\rho_x^2}{2\rho^5} + \cdots \tag{2.9}$$

Taking total time derivatives of $\frac{d}{dt}\int_x x + b\rho(y,t)dy$ from (2.7) shows that the velocity is transformed consistently and that the conservation equation $\rho_t + (\rho v)_x = 0$ holds.

As an example, Berg applies the transformation to a microscopic model (the optimal velocity traffic model developed by Bando *at al* [1] and shown below), and when evaluated against the original results, it produces comparable behaviour. The Bando equation is

$$\frac{dv_i}{dt} = a[U_b \underbrace{(x_{i+1} - x_i)}_{b_i\text{–the headway}} - v_i] \tag{2.10}$$

where the optimal velocity is a function of the distance between the ith and the (i+1)th particle and a is a positive constant. It has been shown by Bando *et al* [1] that the optimal velocity function (optimal in that it is able to reproduce many of the features of real life traffic situations) is

$$U(x) = tanh(x-2) - tanh(2).$$

Applying the transformation gives an expression for the conservation of cars coupled with an approximation of the microscopic equation:

$$\rho_t + (\rho v)_x = 0 \tag{2.11}$$

$$v_t + vv_x = a(V(\rho) - v) + aV'(\rho)\Big(\frac{\rho_x}{2\rho} + \frac{\rho_{xx}}{6\rho^2} - \frac{\rho_x^2}{2\rho^3}\Big) \tag{2.12}$$

with

$$V(\rho) = U_b(\frac{1}{\rho}).$$

Berg shows that there are big efficiency and time savings in solving the macroscopic equation rather than the microscopic one.

Helbing illustrates another approach by defining the average velocity of a car by linear interpolation between the velocities of neighbouring cars and differentiating with respect to time. In [13], he moves from a social force model of traffic dynamics to a macroscopic model using probabilities and calculus to obtain a three equation model of the form

$$\frac{\partial \rho}{\partial t} + \frac{\partial(\rho V)}{\partial r} = 0$$

$$\frac{\partial(\rho V)}{\partial t} + \frac{\partial}{\partial r}[\rho(V^2 + \theta)] = \frac{\rho}{\tau}(V_e^* - V) + \rho\mathcal{F}_1$$

$$\frac{\partial}{\partial t}[\rho(V^2 + \theta)] + \frac{\partial}{\partial r}[\rho(V^3 + 3V\theta)] = \frac{2\rho}{\tau}(V_e^* V + \tau D - V^2 - \theta) + \rho\mathcal{F}_2$$

where ρ = density, r = position, t = time, D = diffusion function, w future velocity $V(r,t)$ = average velocity and $\theta(r,t)$ = velocity variance with

$$\mathcal{F}_k(r,t) = -k\int d\triangle r \int dv \int_{w<v} dw v^{k-1} exp(-\frac{\triangle r - s(v)}{R})\frac{v-w}{\tau'} \times P'(\triangle r, w|r,v,t)P(v;r,t)$$

and

$$V_e^* = \int d\triangle r \int dv \int dw V_e'(\triangle r)P'(\triangle r, w|r,v,t)P(v;r,t)$$

where P denotes a probability.

The next chapter considers some of the numerical methods we will use and then we will use the findings of Berg and Woods to develop the behavioural force model.

Chapter 3

Numerical Methods

3.1 Introduction

When an equation cannot be solved analytically, we can use a variety of numerical methods such as

- finite elements
- finite volumes
- finite differences.

For hyperbolic equations such as conservation laws, finite differences are often used. These aim to construct an approximate solution u^{n+1} at time $n+1$ from previous solutions u^n, u^{n-1} etc depending on the level of the scheme. A typical grid is shown overleaf.

The standard conservation law in one dimension for a system without a source term is

$$\frac{\partial \underline{u}}{\partial t} + \frac{\partial \underline{f}}{\partial x} = 0$$

and $f'(u) = A$ which is the Jacobian matrix. The solution can be approximated numerically by replacing the derivatives with finite difference approximations, taking

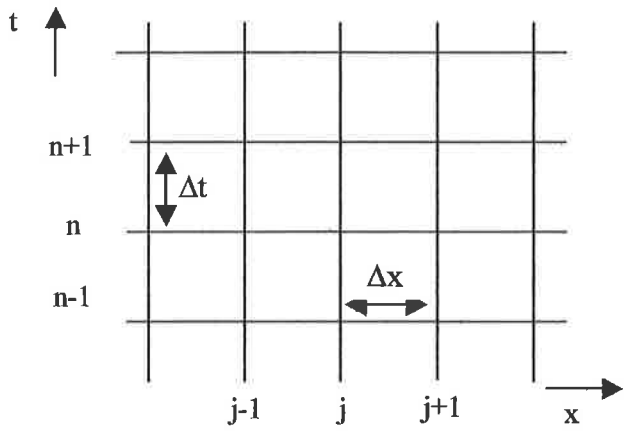

Example Grid

forward, backward or central differences to, hopefully, maximise the accuracy and stability of the scheme. There are two types of scheme:

- explicit - where the current approximation depends only on previous ones, e.g. replacing u_t with a forward in time approximation and u_x with a central in space one gives $\underline{u}_j^{n+1} = \underline{u}_j^n - \frac{\triangle t}{2\triangle x} A(\underline{u}_{j+1}^n - \underline{u}_{j-1}^n)$
- implicit - which has the current approximation on both the left and right hand sides of the equation, e.g. using the central in space approximation at $n+1$ instead of n gives $\underline{u}_j^{n+1} = \underline{u}_j^n - \frac{\triangle t}{2\triangle x} A(\underline{u}_{j+1}^{n+1} - \underline{u}_{j-1}^{n+1})$

For the crowd model we will use a Lax-Friedrichs scheme, an Upwind scheme and a Lax-Wendroff scheme as outlined below.

3.1.1 Truncation Error

The local truncation error measures how well the discrete equation models the differential equation locally. It is derived by replacing the approximate solution in the discrete equation by the true solution, i.e. assuming the values at the grid points are exact, and expanding in a Taylor series. Recall that $u_j^n = u(j\triangle x, n\triangle t)$ and so Taylor

expansions at time n give:

$$u_{j+1}^{n} \approx u(x+\triangle x,t) = u + \triangle x u_x + \frac{\triangle x^2}{2} u_{xx} + \frac{\triangle x^3}{6} u_{xxx} + \dots$$

$$u_{j}^{n+1} \approx u(x,t+\triangle t) = u - \triangle t u_t + \frac{\triangle t^2}{2} u_{tt} + \frac{\triangle t^3}{6} u_{ttt} + \dots$$

Once we collect terms and use the definition of the original equation we are left with an expression for the truncation error in terms of powers of $\triangle t$ and $\triangle x$ (in 1-d). This gives the order of accuracy of the scheme. If the method is stable, the global error is of the same order as the local error. A method is consistent with the differential equation if the truncation error goes to zero as the timestep goes to zero.

3.1.2 Scheme Stability

A scheme is stable if the local error does not grow 'excessively' as each step is applied, i.e the difference between the actual and approximated solution has bounded growth. Le Veque [26] tells us that we can use the Lax Equivalence Theorem to deduce a stability bound for a numerical scheme. The Lax Equivalence Theorem says that for a consistent linear method and a well posed problem, stability is necessary and sufficient for convergence, so if the scheme is stable it will converge to the true solution. Stability holds for a system of equations if

$$|\lambda_i \frac{\triangle t}{\triangle x}| \leq C \tag{3.1}$$

where λ_i are the eigenvalues of the Jacobian matrix A and C is some bound constant. This is known as the CFL condition (after Courant, Friedrichs and Lewy who first devised it) and enables us to choose values of $\triangle t$ so that the scheme remains stable, although it is a necessary and not a sufficient condition for stability.

There are two other types of instability that may arise: instability due to the diffusion term and instability due to the relaxation term. The first may occur when the model has an explicit viscosity term $D\frac{\partial^2 V}{\partial x^2}$ and necessitates an additional diffusional

CFL condition:

$$\frac{D(\triangle x)^2}{2\triangle t} \leq 1$$

Instabilities can also develop when there is a relaxation term as a source term in the model. We will see an example of this later.

3.2 Lax-Friedrichs Method

For the Lax-Friedrichs scheme we use a spatially centred approximation together with a time approximation that averages values at the current timestep to give the explicit scheme:

$$\frac{1}{\triangle t}(\underline{u}_j^{n+1} - \frac{(\underline{u}_{j+1}^n + \underline{u}_{j-1}^n)}{2}) + A(\frac{\underline{u}_{j+1}^n - \underline{u}_{j-1}^n}{2\triangle x}) = 0$$

i.e.

$$\underline{u}_j^{n+1} = \frac{\underline{u}_{j-1}^n + \underline{u}_{j+1}^n}{2} - \frac{\triangle t}{2\triangle x} A(\underline{u}_{j-1}^n - \underline{u}_{j+1}^n).$$

An alternative way of writing this for the general form of the conservative law is

$$\underline{u}_j^{n+1} = \frac{\underline{u}_{j-1}^n + \underline{u}_{j+1}^n}{2} - \frac{\triangle t}{2\triangle x}(\underline{f}_{j+1}^n - \underline{f}_{j-1}^n) \tag{3.2}$$

The truncation error for Lax Friedrich is

$$T_j^n = \frac{\triangle t}{2} u_{tt} - \frac{\triangle x^2}{2\triangle t} u_{xx} + \frac{\triangle x^2}{6}\frac{\partial^3 f}{\partial x^3} + O(\triangle x^3) + O(\triangle t^2) \tag{3.3}$$

and hence Lax-Friedrichs is 1st order in time and 2nd order in space. It has a stability condition of $|\lambda_i \frac{\triangle t}{\triangle x}| \leq 1 \quad \forall i$ where λ_i are the eigenvalues of the Jacobian matrix A.

3.3 Upwind Scheme

The Upwind scheme uses a backward or forward difference in space depending on the sign of the eigenvalue. As we shall see, the eigenvalues for our model are both positive in one dimension and so we only need to use a one sided scheme:

$$\underline{u}_j^{n+1} = \underline{u}_j^n - \frac{\triangle t}{\triangle x}(\underline{f}_j^n - \underline{f}_{j-1}^n). \tag{3.4}$$

It has a truncation error

$$T_j^n = \frac{\triangle t}{2} u_{tt} + \frac{\triangle x}{2} f(u)_{xx} + O(\triangle x^2) + O(\triangle t^2) \tag{3.5}$$

and therefore is 1st order in time and space. The Upwind scheme has an interval of stability $\lambda_i \frac{\triangle t}{\triangle x} \leq 1$.

3.4 Lax-Wendroff

Lax-Wendroff is one of the most well known second order schemes and for the linear hyperbolic equation $\frac{\partial u}{\partial t} + A\frac{\partial u}{\partial x} = 0$ takes the form [26]

$$\underline{u}_j^{n+1} = \underline{u}_j^n - \frac{\triangle t}{2\triangle x} A(\underline{u}_{j+1}^n - \underline{u}_{j-1}^n) + \frac{\triangle t^2}{2\triangle x^2}(\underline{u}_{j+1}^n - 2\underline{u}_j^n + \underline{u}_{j-1}^n) \tag{3.6}$$

which is derived from a Taylors series expansion and the relationship $\frac{\partial^2 u}{\partial t^2} = A^2 \frac{\partial^2 u}{\partial x^2}$. Taking centred difference approximations for the derivatives and rearranging gives (3.6).

For a nonlinear conservation law $A(u) = f'(u)$ is the Jacobian matrix and so the scheme becomes

$$\underline{u}_j^{n+1} = \underline{u}_j^n - \frac{\triangle t}{2\triangle x}(\underline{f}(u_{j+1}^n) - \underline{f}(u_{j-1}^n)) + \frac{\triangle t^2}{2\triangle x^2}\Big(A_{j+\frac{1}{2}}(\underline{f}(u_{j+1}^n) - \underline{f}(u_j^n)) - A_{j-\frac{1}{2}}(\underline{f}(u_j^n) - \underline{f}(u_{j-1}^n))\Big) \tag{3.7}$$

However we can avoid having to calculate the Jacobian matrix by using the Richtmyer two step Lax-Wendroff method:

$$\underline{u}_{j+\frac{1}{2}}^{n+\frac{1}{2}} = \frac{1}{2}(\underline{u}_j^n + \underline{u}_{j+1}^n) - \frac{\triangle t}{2\triangle x}(\underline{f}(u_{j+1}^n) - \underline{f}(u_j^n))$$

$$\underline{u}_j^{n+1} = \underline{u}_j^n - \frac{\triangle t}{\triangle x}(\underline{f}(u_{j+\frac{1}{2}}^{n+\frac{1}{2}}) - \underline{f}(u_{j-\frac{1}{2}}^{n+\frac{1}{2}})). \tag{3.8}$$

For the linear equation (3.6) we can show Lax-Wendroff has a truncation error of

$$\frac{1}{6}\Big(\triangle t^2 \frac{\partial^3 u}{\partial t^3} - A\triangle x^2 \frac{\partial^3 u}{\partial x^3}\Big) + O(\triangle x^3) + O(\triangle t^3) \tag{3.9}$$

and hence is second order in both time and space. The interval of stability for the scheme is the same as for Lax-Friedrichs.

3.5 Source Terms

For our system of equations we will need to deal with source terms on the right hand side, i.e.

$$\frac{\partial \underline{u}}{\partial t} + \frac{\partial \underline{f}}{\partial x} = \underline{s}(u)$$

Numerically the easiest way to deal with the source term is to add it to any of the schemes outlined multiplied by $\triangle t$. So, for example, Lax-Friedrichs becomes

$$\underline{u}_j^{n+1} = \frac{\underline{u}_{j-1}^n + \underline{u}_{j+1}^n}{2} - \frac{\triangle t}{2\triangle x}(\underline{f}_{j+1}^n - \underline{f}_{j-1}^n) + \triangle t \underline{s}_j^n$$

For more details on alternative ways of dealing with source terms see [17].

3.6 Modified Equation

To look at the behaviour of solutions in more detail, one approach is to model the numerical equation by a differential equation [26]. This often results in a PDE which is solved more accurately than the original equation being modelled (the 'modified' equation), highlighting additional terms which may affect the solution. For example, the modified equation for Lax-Friedrichs, found by similar analysis to that used to find truncation errors, where $u(x,t)$ is taken to be the exact solution to $u_t + Au_x = 0$ is

$$\underline{u}_t + A\underline{u}_x + \frac{1}{2}(\triangle t \underline{u}_{tt} - \frac{\triangle x^2}{\triangle t}\underline{u}_{xx}) = 0$$

which would have a truncation error of order $(\triangle t)^2$ and hence we would get a more accurate solution to this than our original equation. Expressing u_{tt} in terms of x derivatives gives

$$\underline{u}_t + A\underline{u}_x = \frac{(\triangle x)^2}{2\triangle t}\Big(I - \frac{(\triangle t)^2 A^2}{(\triangle x)^2}\Big)\underline{u}_{xx}, \tag{3.10}$$

an advection diffusion equation where the diffusion term will cause solutions to become smeared out as time evolved. For the Upwind scheme the modified equation

is

$$\underline{u}_t + A\underline{u}_x = \frac{1}{2}\triangle x A\Big(I - \frac{\triangle t A}{\triangle x}\Big)\underline{u}_{xx}, \tag{3.11}$$

also an advection diffusion equation but here the scheme would be less diffusive. For both, the equations are well posed only if the eigenvalues of the diffusion coefficient matrix, D (multiplying the u_{xx} term), are non negative. This also leads to the stability criteria derived earlier. The Lax Wendroff scheme gives a 3rd order accurate approximation to the modified equation

$$\underline{u}_t + A\underline{u}_x = \frac{(\triangle x)^2}{6}\Big(\frac{(\triangle t)^2 A^2}{(\triangle x)^2} - I\Big)\underline{u}_{xx}, \tag{3.12}$$

which is a dispersive equation. This leads to the oscillatory behaviour typical of Lax Wendroff, with slow wave numbers causing lagging oscillations behind discontinuties.

3.7 2-D Equations and Dimensional Splitting

In two dimensions, conservation laws take the form

$$\frac{\partial \underline{u}}{\partial t} + \frac{\partial \underline{f}}{\partial x} + \frac{\partial \underline{g}}{\partial y} = 0 \tag{3.13}$$

One approach to solving this numerically is to use any of the discrete one-dimensional methods and apply them alternately on one-dimensional problems in the x and y directions [4] [28]. For (3.13) with initial condition $\underline{u}(x, y, t^n) = \underline{u}^n$, and denoting the average of $\underline{u}(x, y, t^n)$ in each cell by u^n_{ij}, we take an 'x-sweep'

$$\frac{\partial \underline{u}}{\partial t} + \frac{\partial \underline{f}}{\partial x} = 0 \qquad \Rightarrow \qquad \underline{u}^{n+\frac{1}{2}}$$

and then use this as the initial value for a 'y-sweep' to take it to a full timestep.

$$\frac{\partial \underline{u}}{\partial t} + \frac{\partial \underline{f}}{\partial y} = 0 \qquad \Rightarrow \qquad \underline{u}^{n+1}$$

Any source terms can be dealt with in the same way. If the individual 1-D sweep schemes are first order accurate then the sweep strategy is also first order accurate. Similarly if the 1-D schemes are second order accurate, this is carried through.

There are other ways of splitting the timesteps to improve the accuracy of the scheme [29]. For example to obtain second order accuracy the splitting coefficients would be 0.25, 0.5 and 0.25.

Chapter 4

A One Dimensional Crowd!

4.1 Introduction

Obviously crowds are not one-dimensional. However to initially test our approach we will consider a one-dimensional flow of people for example along a corridor. (see diagram overleaf)

4.2 A 1-D Model

Consider the behavioural force model decribed in Chapter 2:

$$\frac{dv_i(t)}{dt} = \frac{v_i^0(t)e_i^0(t)}{\tau_i} + \frac{\xi_i(t) - v_i(t)}{\tau_i} + f_{ij}^{soc}(t) + f_{ij}^{ph}(t) + f_{ij}^{b}. \tag{4.1}$$

We can simplify it with the following assumptions:

- people are not panicking and do not bump into each other, i.e. we can disregard $f_{ij}^{ph}(t)$
- people do not interact with the boundaries, i.e. ignore f_{ij}^{b}
- $\lambda_{ij} = 0$ so interactions are isotropic.

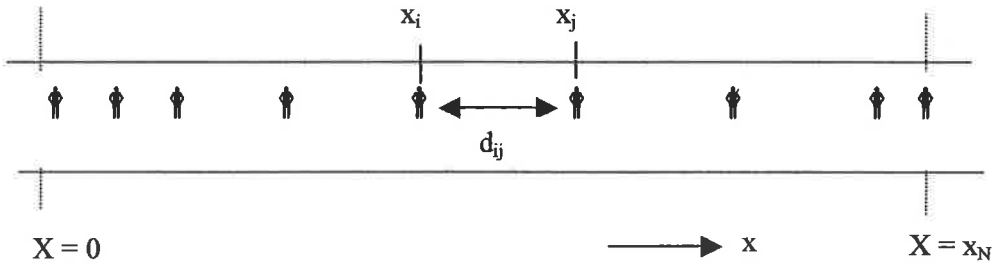

A One-Dimensional Crowd

Then our microscopic equation becomes

$$\frac{dv_i(t)}{dt} = \frac{v_i^0(t)e_i^0(t) - v_i(t)}{\tau_i} + A_i exp(\frac{r_{ij} - d_{ij}}{B_{ij}})n_{ij}\frac{1 + cos\psi_{ij}}{2}.$$

In one dimension, people are moving in a straight line and so $cos\psi_{ij} = 1$ and $n_{ij} = -1$ (as it points from pedestrian j to i), so we have

$$\frac{dv_i(t)}{dt} = \frac{v_i^0(t)e_i^0(t) - v_i(t)}{\tau_i} - A_i exp(\frac{r_{ij} - d_{ij}}{B_{ij}}). \tag{4.2}$$

Berg and Woods' conversion depends on linking the headway b to the density and so for a pedestrian model we need to define an equivalent relationship. One option is to take the distance between two pedestrians in a crowd given by d_{ij} (= the distance between the centres of mass of pedestrians i and j), and hence define

$$d_{ij} \sim \frac{1}{\rho} - \frac{\rho_x}{2\rho^3} - \frac{\rho_{xx}}{6\rho^4} + \frac{\rho_x^2}{2\rho^5}. \tag{4.3}$$

For ease of calculation, we can express (4.2) as:

$$\frac{dv_i(t)}{dt} = \frac{v_i^0(t)e_i^0(t) - v_i(t)}{\tau_i} - f(d) \tag{4.4}$$

where $f(d) = A_i exp(\frac{r_{ij} - d_{ij}}{B_{ij}})$ is a function of pedestrian 'headway'. Substituting 4.3 into 4.4 gives

$$\frac{dv_i(t)}{dt} = \frac{v_i^0(t)e_i^0(t) - v_i(t)}{\tau_i} - f(\frac{1}{\rho} - \frac{\rho_x}{2\rho^3} - \frac{\rho_{xx}}{6\rho^4} + \frac{\rho_x^2}{2\rho^5}). \tag{4.5}$$

Expanding the term in brackets in a Taylor Series around $\frac{1}{\rho}$ and truncating gives

$$\frac{dv_i(t)}{dt} = \frac{v_i^0(t)e_i^0(t) - v_i(t)}{\tau_i} - f(\frac{1}{\rho}) - (\frac{\rho_x}{2\rho^3} + \frac{\rho_{xx}}{6\rho^4} - \frac{\rho_x^2}{2\rho^5})f'(\frac{1}{\rho}).$$

Now, in a similar way to Berg and Woods [2] we can set $f(\frac{1}{\rho}) = \overline{f}(\rho)$ and $f'(\frac{1}{\rho}) = -\rho^2\overline{f}'(\rho)$ to give

$$v_t + vv_x = \frac{v_i^0 e_i^0 - v_i}{\tau_i} - \overline{f}(\rho) + \overline{f}'(\rho)(\frac{\rho_x}{2\rho} + \frac{\rho_{xx}}{6\rho^2} - \frac{\rho_x^2}{2\rho^3}). \tag{4.6}$$

For a macroscopic model we can take average values for the constants v^0, e^0 and τ. Multiplying equation (4.6) by ρ and using the conservation law gives

$$\frac{\partial}{\partial t}(\rho v) + \frac{\partial}{\partial x}(\rho v^2) = \frac{(v^0e^0 - v)\rho}{\tau_{ave}} - \rho\overline{f}(\rho) - \overline{f}'(\rho)(\frac{\rho_x}{2} + \frac{\rho_{xx}}{6\rho} - \frac{\rho_x^2}{2\rho^2}).$$

From (4.4), substituting back

$$f(\frac{1}{\rho}) = \overline{f}(\rho) = Aexp(\frac{R\rho^2 - 1}{B\rho})$$

$$\overline{f}'(\rho) = A\frac{R\rho^2 + 1}{B\rho^2}exp(\frac{R\rho^2 - 1}{B\rho})$$

where r_{ij} is taken to be equivalent to an occupancy term in traffic [27] and can be defined as $r = R_{ave}\rho$ with R_{ave} the average radius of a person and ρ the density.

So we get a system of conservation equations, analogous to (2.11) and (2.12):

$$\frac{\partial \rho}{\partial t} + \frac{\partial}{\partial x}(\rho v) = 0 \tag{4.7}$$

$$\frac{\partial}{\partial t}(\rho v) + \frac{\partial}{\partial x}(\rho v^2) = \frac{(v^0e^0 - v)\rho}{\tau_{ave}} - A\rho exp(\frac{R\rho^2 - 1}{B\rho}) - \frac{A(R\rho^2 + 1)}{B\rho^2}(\frac{\rho_x}{2} + \frac{\rho_{xx}}{6\rho} - \frac{\rho_x^2}{2\rho^2})exp(\frac{R\rho^2 - 1}{B\rho}) \tag{4.8}$$

In order to use the equations we need to define values for the constants:

- interaction strength A varies between 0 and 1
- initial desired velocity v^0 is taken to be equal to the mean value 1.34m/s
- the average radius of a person is taken to be 0.3m based on Fruin data

National guidance suggests that critical density is one person per square metre with the safety limit for crowds being 40 people per 10 square metres [23]. In a one-dimensional case, it would be physically impossible to have a maximum density much greater than 4. So from (4.7) and (4.8), letting $\rho v = Q$ we have:

$$\frac{\partial \rho}{\partial t} + \frac{\partial Q}{\partial x} = 0 \tag{4.9}$$

$$\frac{\partial Q}{\partial t} + \frac{\partial Q^2/\rho}{\partial x} = \frac{v^0 e^0 \rho - Q}{\tau_{ave}} - A\rho exp\Big(\frac{R\rho^2 - 1}{B\rho}\Big) - \frac{A(R\rho^2+1)}{B\rho^2}\Big(\frac{\rho_x}{2} + \frac{\rho_{xx}}{6\rho} - \frac{\rho_x^2}{2\rho^2}\Big)exp\Big(\frac{R\rho^2-1}{B\rho}\Big). \tag{4.10}$$

For the second equation, splitting the derivative terms gives:

$$\frac{\partial Q}{\partial t} + \frac{\partial Q^2/\rho}{\partial x} = \frac{v^0 e^0 \rho - Q}{\tau_{ave}} - A\rho exp\Big(\frac{R\rho^2-1}{B\rho}\Big) - \frac{A(R\rho^2+1)}{B\rho^2}\Big(\frac{\rho_{xx}}{6\rho} - \frac{\rho_x^2}{2\rho^2}\Big)exp\Big(\frac{R\rho^2-1}{B\rho}\Big) - \frac{A(R\rho^2+1)\rho_x}{2B\rho^2}exp\Big(\frac{R\rho^2-1}{B\rho}\Big). \tag{4.11}$$

Integrating the last term and gathering $\frac{\partial}{\partial x}$ terms onto the left hand side:

$$\frac{\partial Q}{\partial t} + \frac{\partial}{\partial x}\Big(\frac{Q^2}{\rho} + \frac{A}{2}exp\Big(\frac{R\rho^2-1}{B\rho}\Big)\Big) = \frac{v^0 e^0 \rho - Q}{\tau_{ave}} - A\rho exp\Big(\frac{R\rho^2-1}{B\rho}\Big) - \frac{A(R\rho^2+1)}{B\rho^2}\Big(\frac{\rho_{xx}}{6\rho} - \frac{\rho_x^2}{2\rho^2}\Big)exp\Big(\frac{R\rho^2-1}{B\rho}\Big). \tag{4.12}$$

So we have

$$\underline{u} = (\rho, Q)^T$$

$$\underline{f} = \Big(Q, \frac{Q^2}{\rho} + \frac{A}{2}exp\Big(\frac{R\rho^2-1}{B\rho}\Big)\Big)^T$$

$$\underline{s} = \Big(0, \frac{v^0 e^0 \rho - Q}{\tau_{ave}} - A\rho exp\Big(\frac{R\rho^2-1}{B\rho}\Big) - \frac{A(R\rho^2+1)}{B\rho^2}\Big(\frac{\rho_{xx}}{6\rho} - \frac{\rho_x^2}{2\rho^2}\Big)exp\Big(\frac{R\rho^2-1}{B\rho}\Big)\Big)^T$$

To calculate the region of stability we need to look at the eigenvalues of $\frac{\partial f}{\partial u}$ (see section 3.1):

$$A = \frac{\partial f}{\partial u} = \begin{pmatrix} 0 & 1 \\ -\frac{Q^2}{\rho^2} + \frac{A(R\rho^2+1)}{2B\rho^2}exp\big(\frac{R\rho^2-1}{B\rho}\big) & \frac{2Q}{\rho} \end{pmatrix}$$

and so

$$|A - \lambda I| = \begin{vmatrix} -\lambda & 1 \\ -\frac{Q^2}{\rho^2} + \frac{A(R\rho^2+1)}{2B\rho^2}exp\big(\frac{R\rho^2-1}{B\rho}\big) & \frac{2Q}{\rho} - \lambda \end{vmatrix} = 0$$

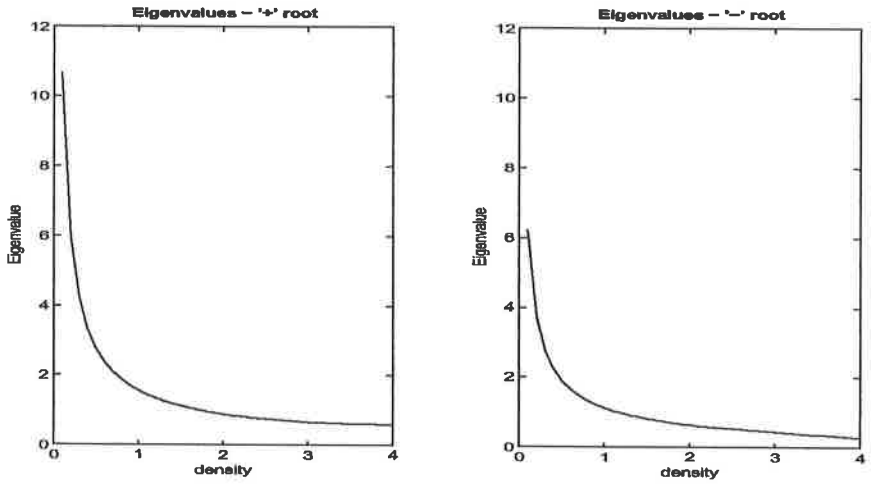

Figure 4.1: Eigenvalues for the 1-D Model

$$\lambda_i = \frac{Q}{\rho} \pm \sqrt{\frac{A(R\rho^2+1)}{2B\rho^2} exp(\frac{R\rho^2-1}{B\rho})}. \tag{4.13}$$

Hence the stability criteria is

$$\Delta t < |\frac{\Delta x}{\frac{Q}{\rho} \pm \sqrt{\frac{A(R\rho^2+1)}{2B\rho^2} exp(\frac{R\rho^2-1}{B\rho})}}|.$$

The sign of the eigenvalues clearly depends on the size of the respective terms. For realistic scenarios, density will range from 0 to about 4. Plotting the eigenvalues shows (see Figure 4.2) that both are positive.

4.3 Numerics

From (4.9) and (4.12) we have a system of equations modelling one dimensional crowd behaviour:

$$\frac{\partial \rho}{\partial t} + \frac{\partial Q}{\partial x} = 0 \tag{4.14}$$

$$\frac{\partial Q}{\partial t} + \frac{\partial}{\partial x}(\frac{Q^2}{\rho} + \frac{A}{2} exp(\frac{R\rho^2-1}{B\rho})) = \frac{v^0 e^0 \rho - Q}{\tau_{ave}} - A\rho exp(\frac{R\rho^2-1}{B\rho}) - \frac{A(R\rho^2+1)}{B\rho^2}(\frac{\rho_{xx}}{6\rho} - \frac{\rho_x^2}{2\rho^2}) exp(\frac{R\rho^2-1}{B\rho}). \tag{4.15}$$

Applying any numerical scheme to this involves dealing with a complicated source term

$$\underline{s} = (0, \frac{v^0 e^0 \rho - Q}{\tau_{ave}} - A\rho exp(\frac{R\rho^2 - 1}{B\rho}) - \frac{A(R\rho^2 + 1)}{B\rho^2}(\frac{\rho_{xx}}{6\rho} - \frac{\rho_x^2}{2\rho^2})exp(\frac{R\rho^2 - 1}{B\rho}))^T$$

which numerically gives rise to two problems:

- how to deal with the derivative terms
- the impact of the relaxation term.

For the first, this was overcome by approximating each derivative directly and solving as an integral part of the system. Using central second differences for $\frac{\rho_{xx}}{6\rho}$, and an upwind multiplied by a downwind scheme for $\frac{\rho_x^2}{2\rho^2}$ gives

$$(\frac{\rho_{xx}}{6\rho} - \frac{\rho_x^2}{2\rho^2}) = \frac{1}{6\rho_j^n}\frac{\rho_{j+1}^n - 2\rho_j^n + \rho_{j-1}^n}{(\triangle x)^2} - \frac{1}{2(\rho^2)_j^n}(\frac{\rho_j^n - \rho_{j-1}^n}{\triangle x})(\frac{\rho_{j+1}^n - \rho_j^n}{\triangle x}). \qquad (4.16)$$

This results in an additional stability criteria

max(differentiation of RHS) $\triangle t < 2$.

The impact of the relaxation term caused more signficant problems, resulting (for example when approximated using Lax-Friedrichs) in wild oscillations (see Figure 4.3) This implies that this part of the source term is stiff i.e. to maintain numerical stability the timestep needs to be far smaller for the relaxation term than for the rest of the system. However, whilst the system could be stabilised using a very small timestep throughout this is impractical as to make any progress in the model the number of steps needed would be very large. With a relaxation time of 0.5 seconds and $\triangle x$=1, $\triangle t$=0.00001 is needed to maintain stability, requiring 30,000 timesteps to even reach a minute. (For further information on stiff source terms see [22] or [25]). To overcome this, the numerical approximation occurred in two stages: firstly, an explicit scheme (i.e. Lax-Friedrichs or Upwind) was applied to (4.9) without the relaxation term included, and then an implicit scheme was used on the relaxation term alone. As implicit schemes are unconditionally stable the above oscillatory problems do not occur. The Trapezium method was used.

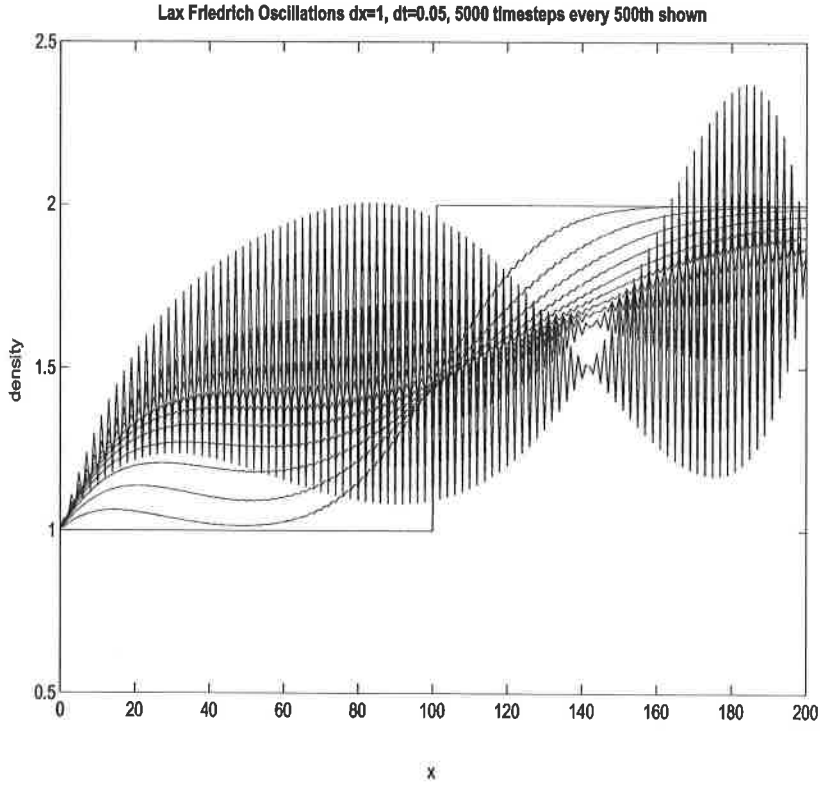

Figure 4.2: Oscillations using Lax-Friedrichs when including relaxation term

4.3.1 Applying the schemes

We apply the Lax-Friedrichs, Upwind and Lax-Wendroff schemes to

$$\frac{\partial \rho}{\partial t} + \frac{\partial Q}{\partial x} = 0 \tag{4.17}$$

$$\frac{\partial Q}{\partial t} + \frac{\partial}{\partial x}(\frac{Q^2}{\rho} + \frac{A}{2} exp(\frac{R\rho^2 - 1}{B\rho})) = \frac{v^0 e^0 \rho - Q}{\tau_{ave}} - A\rho exp(\frac{R\rho^2 - 1}{B\rho}) - \frac{A(R\rho^2 + 1)}{B\rho^2}(\frac{\rho_{xx}}{6\rho} - \frac{\rho_x^2}{2\rho^2}) exp(\frac{R\rho^2 - 1}{B\rho}). \tag{4.18}$$

Lax-Friedrichs

We saw from Chapter 3 that a conservation equation with a source term

$$\frac{\partial \underline{u}}{\partial t} + \frac{\partial \underline{\underline{f}}}{\partial x} = \underline{s}$$

can be approximated by the Lax Friedrich scheme

$$\underline{u}_j^{n+1} = \frac{\underline{u}_{j-1}^n + \underline{u}_{j+1}^n}{2} - \frac{\triangle t}{2\triangle x}(\underline{f}_{j+1}^n - \underline{f}_{j-1}^n) + \triangle t \underline{s}_j^n.$$

So applying it to (4.18) gives the system

$$\rho_j^{n+1} = \frac{\rho_{j-1}^n + \rho_{j+1}^n}{2} - \frac{\triangle t}{2\triangle x}(Q_{j+1}^n - Q_{j-1}^n) \tag{4.19}$$

$$\begin{aligned} Q_j^{n+1} = \frac{Q_{j-1}^n + Q_{j+1}^n}{2} - \frac{\triangle t}{2\triangle x}\Big(((\frac{Q^2}{\rho})_{j+1}^n + \frac{A}{2}exp(\frac{R(\rho^2)_{j+1}^n - 1}{B\rho_{j+1}^n})) - ((\frac{Q^2}{\rho})_{j-1}^n + \\ + \frac{A}{2}exp(\frac{R(\rho^2)_{j-1}^n - 1}{B\rho_{j-1}^n}))\Big) + \triangle t(-A\rho_j^n exp(\frac{R(\rho^2)_j^n - 1}{B\rho_j^n}) - \frac{A(R(\rho^2)_j^n + 1)}{B(\rho^2)_j^n} \\ (\frac{1}{6\rho_j^n}\frac{\rho_{j+1}^n - 2\rho_j^n + \rho_{j-1}^n}{(\triangle x)^2} - \frac{1}{2(\rho^2)_j^n}(\frac{\rho_j^n - \rho_{j-1}^n}{\triangle x})(\frac{\rho_{j+1}^n - \rho_j^n}{\triangle x}))exp(\frac{R(\rho^2)_j^n - 1}{B\rho_j^n})) \end{aligned}$$

Upwind

The Upwind scheme is

$$\underline{u}_j^{n+1} = \underline{u}_j^n - \frac{\triangle t}{\triangle x}(\underline{f}_j^n - \underline{f}_{j-1}^n) + \triangle t \underline{s}_j^n.$$

Applied to (4.18) gives

$$\rho_j^{n+1} = \rho_j^n - \frac{\triangle t}{\triangle x}(Q_j^n - Q_{j-1}^n) \tag{4.20}$$

$$\begin{aligned} Q_j^{n+1} = Q_j^n - \frac{\triangle t}{\triangle x}\Big(((\frac{Q^2}{\rho})_j^n + \frac{A}{2}exp(\frac{R(\rho^2)_j^n - 1}{B\rho_j^n})) - ((\frac{Q^2}{\rho})_{j-1}^n + \\ + \frac{A}{2}exp(\frac{R(\rho^2)_{j-1}^n - 1}{B\rho_{j-1}^n}))\Big) + \triangle t(-A\rho_j^n exp(\frac{R(\rho^2)_j^n - 1}{B\rho_j^n}) - \\ - \frac{A(R(\rho^2)_j^n + 1)}{B(\rho^2)_j^n}(\frac{1}{6\rho_j^n}\frac{\rho_{j+1}^n - 2\rho_j^n + \rho_{j-1}^n}{(\triangle x)^2} - \frac{1}{2(\rho^2)_j^n}(\frac{\rho_j^n - \rho_{j-1}^n}{\triangle x})(\frac{\rho_{j+1}^n - \rho_j^n}{\triangle x})exp(\frac{R(\rho^2)_j^n - 1}{B\rho_j^n})) \end{aligned}$$

Lax-Wendroff

The two step Lax-Wendroff scheme

$$\underline{u}_{j+\frac{1}{2}}^{n+\frac{1}{2}} = \frac{1}{2}(\underline{u}_j^n + \underline{u}_{j+1}^n) - \frac{\triangle t}{2\triangle x}(\underline{f}(u_{j+1}^n) - \underline{f}(u_j^n)) + \triangle t \underline{s}_j^n.$$

$$\underline{u}_j^{n+1} = \underline{u}_j^n - \frac{\triangle t}{\triangle x}(\underline{f}(u_{j+\frac{1}{2}}^{n+\frac{1}{2}}) - \underline{f}(u_{j-\frac{1}{2}}^{n+\frac{1}{2}})) + \triangle t \underline{s}_j^n \tag{4.21}$$

applied to (4.18) gives

Step 1

$$\rho_{j+\frac{1}{2}}^{n+\frac{1}{2}} = \frac{1}{2}(\rho_j^n + \rho_{j+1}^n) - \frac{\triangle t}{2\triangle x}(Q_{j+1}^n - Q_j^n) \tag{4.22}$$

$$Q_{j+\frac{1}{2}}^{n+\frac{1}{2}} = \frac{1}{2}(Q_j^n + Q_{j+1}^n) - \frac{\triangle t}{2\triangle x}(((\frac{Q^2}{\rho})_{j+1}^n + \frac{A}{2}exp(\frac{R(\rho^2)_{j+1}^n - 1}{B\rho_{j+1}^n})) - ((\frac{Q^2}{\rho})_j^n + \frac{A}{2}exp(\frac{R(\rho^2)_j^n - 1}{B\rho_j^n})))$$

Step2

$$\rho_j^{n+1} = \rho_j^n - \frac{\triangle t}{\triangle x}(Q_{j+\frac{1}{2}}^{n+\frac{1}{2}} - Q_{j+\frac{1}{2}}^{n+\frac{1}{2}}) \tag{4.23}$$

$$Q_j^{n+1} = Q_j^n - \frac{\triangle t}{\triangle x}\Big(((\frac{Q^2}{\rho})_{j+\frac{1}{2}}^{n+\frac{1}{2}} + \frac{A}{2}exp(\frac{R(\rho^2)_{j+\frac{1}{2}}^{n+\frac{1}{2}} - 1}{B\rho_{j+\frac{1}{2}}^{n+\frac{1}{2}}})) - - ((\frac{Q^2}{\rho})_{j-\frac{1}{2}}^{n+\frac{1}{2}} + \frac{A}{2}exp(\frac{R(\rho^2)_{j-\frac{1}{2}}^{n+\frac{1}{2}} - 1}{B\rho_{j-\frac{1}{2}}^{n+\frac{1}{2}}}))\Big)$$

and for the source term

$$Q_j^{n+1} = Q_j^n + \triangle t s(\rho_j^n, Q_j^n). \tag{4.24}$$

Trapezium

Each of these is coupled with the implicit Trapezium method for the relaxation term, i.e.

$$\frac{\rho_j^{n+1} - \rho_j^n}{\triangle t} = 0 \qquad \Rightarrow \qquad \rho_j^{n+1} = \rho_j^n$$

$$\frac{Q_j^{n+1} - Q_j^n}{\triangle t} = \frac{1}{2\tau}(v^0 e^0(\rho_j^{n+1} + \rho_j^n) - (Q_j^{n+1} + Q_j^n)) \quad \Rightarrow \quad Q_j^{n+1} = Q_j^n(\frac{1/\triangle t - 1/2\tau}{1/\triangle t + 2\tau}) + \frac{1/\tau v^0 e^0 \rho_j^n}{1/\triangle t + 2\tau}.$$

4.3.2 Initial and Boundary Conditions

To calculate pedestrian flows we need to calculate initial and boundary conditions. From the work of Helbing and Togawa we know that

- desired velocity for pedestrians has mean 1.34m/s and standard deviation 0.26m/s
- velocity can be related to density by $v = v_0\rho^{-0.8}$ where $v_0 = 1.34$ (Figure 4.3)

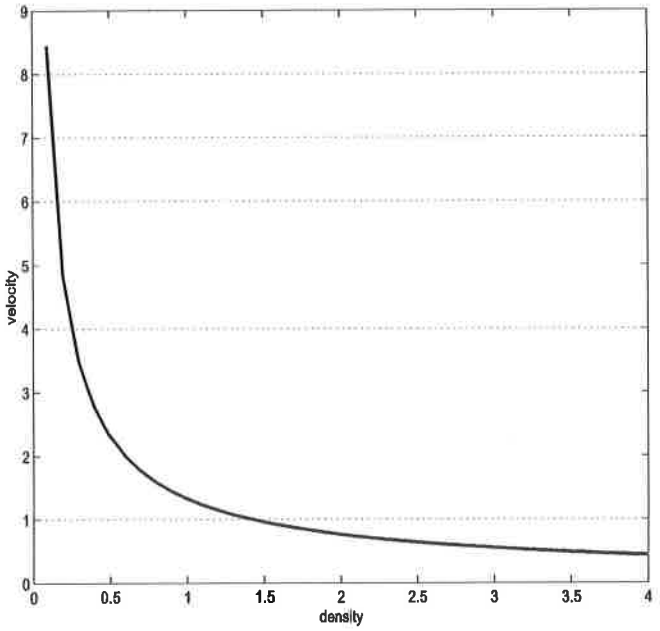

Figure 4.3: Initial relationship between velocity and density according to Togawa formula

These are used to relate different initial conditions. We will look at a number of different scenarios:

- steady flow
- a low constant density increasing suddenly to high constant density
- a high constant density decreasing suddenly to low constant density

- slowly increasing and decreasing densities

Obviously sudden changes in density are not that realistic in 1-D as they may involve people disappearing or appearing through a trapdoor or hole in the ground, or ending up in clinches, but these scenarios allow us to compare numerical results.

Boundary conditions allow us to look at how the model progresses under different circumstances. There are many different types of boundary conditions but the main ones are:

- Dirichlet boundary conditions where values are given at $\underline{u}(0,t)$ and $\underline{u}(L,t)$ where L is the length of the corridor.
- Von Neumann boundary conditions where flow at the boundary remains unchanged $\frac{\partial u}{\partial x}(0,t) = \frac{\partial u}{\partial x}(L,t) = 0$
- free / smooth boundary conditions where $\frac{\partial^2 u}{\partial x^2}(0,t) = \frac{\partial^2 u}{\partial x^2}(L,t) = 0$

For our model we could use:

- periodic boundary conditions
- constant boundary conditions allowing for a steady stream of people into the corridor
- a zero velocity boundary condition at the right hand end to simulate a blockage or wall.

4.4 Results

Unless otherwise stated, results are based on timesteps of 0.02 seconds, spatial steps of 1 metre and a 1-D 'corridor' of length 250 metres. Results are run for 9000 timesteps (3 minutes) and every 500th timestep is shown.

4.4.1 Steady Flow

Considering both constant initial and boundary conditions shows typical properties of the three numerical schemes. This mirrors the unexciting situation of everyone at a constant density with a steady flow of 1 person continually moving into the scenario. Lax-Friedrichs (Figure 4.4) produces results showing that the stream of people will gradually settle to a constant density of 1: the initial fastest moving people will move out the space of interest and the arrivals will continue at constant speed, maintaining their distance from others and not speeding up. However, although this can be explained away, it could be more to do with the diffusive properties of the numerical scheme than physical behaviour. Particularly as the boundary conditions force a flattening of the results, the reduction in density could be numerically more pronounced than it would be physically. Applying the Upwind scheme to an identical problem (Figure 4.5) does not give the same diffusion: it gives a much sharper profile where people arrive at a density of one per metre but then quickly increase their speed to match the initial density profile. An even sharper profile is given by Lax-Wendroff (Figure 4.6) although with the typical trailing edge oscillations.

4.4.2 Increasing initial density

Figures 4.7 to 4.16 show results for an initial increase in density where

$$\rho(x,0) = \begin{cases} 0.5 & \text{if } x \leq 100 \\ 0.015x - 1 & \text{if } 100 < x < 200 \\ 2.0 & \text{if } x \geq 200. \end{cases}$$

Figure 4.7 considers the effects of varying values of α, the interaction strength, whilst keeping $\triangle t$ and $\triangle x$ fixed using Lax-Friedrichs. The graph shows that the density reduces more slowly as the interaction strength increases. Results were also calculated varying $\triangle x$ with constant $\triangle t$ and showed that this makes little difference

unless $\triangle x$ is small. At $\triangle x = 0.1$, the system becomes unstable after about 25 seconds and needs a smaller timestep.

Figure 4.8 shows an increasing density profile with a constant density feeding into the beginning of the corridor at 0.5 people / metre. Again Lax-Friedrichs shows diffusive effects where, physically, we would hope people would speed up. The Upwind (Figure 4.10) and Lax-Wendroff (Figure 4.11) schemes show this speeding up effect with people coming in able to increase their speed to minimise the time taken to reach the far end of the corridor.

Figures 4.12 and 4.13 model zero velocity at the far end of the corridor. This is a crude way of simulating a sudden pile up although may cause the problem to become analytically ill-posed. Further work is needed on this effect, as the second derivative term in the source equation may impact on this. Lax-Friedrichs mirrors the pile up well. Obviously any density above about 4 would result in injury and crushing. A practical model would limit the maximum density but we just aim to highlight the nature of the behaviour. The upwind scheme does not really capture the 'pile up', with an increase in density occuring very suddenly right at the end. As the upwind scheme only depends on the current and previous positions, the boundary condition is not fed back into the process and only affects the last value. Unlike the central Lax-Friedrichs scheme where both left and right numerical boundary conditions are needed, the right hand boundary condition for the Upwind is unnecessary. Trying to model the same situation with Lax-Wendroff causes instability. Figures 4.14 to 4.16 show a less severe scenario where velocity at the end point is half that at the end at the previous timestep. Lax-Friedrichs models best what would be expected with an increasing density, Upwind again does not feed the information back into the profile but Lax-Wendroff, whilst not breaching its stability criteria, begins to oscillate wildly.

4.4.3 Decreasing initial density

Figures 4.17 to 4.24 show results for an initial decrease in density where

$$\rho(x,0) = \begin{cases} 2.5 & \text{if } x \leq 100 \\ 4.5 - 0.02x & \text{if } 100 < x \leq 150 \\ 1.5 & \text{if } 150 < x \leq 200 \\ 7.5 - 0.03x & \text{if } 200 < x < 250 \\ 0.01 & \text{if } x = 250. \end{cases}$$

and people flow in at a constant density of 1.

Similar effects to before are observed. For Lax-Wendroff (Figures 4.19 and 4.20) people come in at constant speed but do speed up, although taking longer and longer to do so. With decreasing density, Lax-Friedrichs again simulates 'pile up' situations (Figures 4.21 and 4.22). Lax-Wendroff shows some interesting bifurcation type behaviour, oscillating between two values towards the end of the corridor. Bifurcation occurs when one eigenvalue becomes zero and equilibrium states collide.

4.4.4 Simulating a blockage

Figures 4.25 to 4.27 show, for each of the initial condition scenarios, what happens when a 'blockage' occurs along the corridor. For the area 170-175 metres, the velocity is defined as half of the velocity at the previous timestep (rather than zero so the blockage is not insurmountable). Lax-Friedrichs is used and shows an increase in density as expected, followed by a recovery period to go back to a constant density.

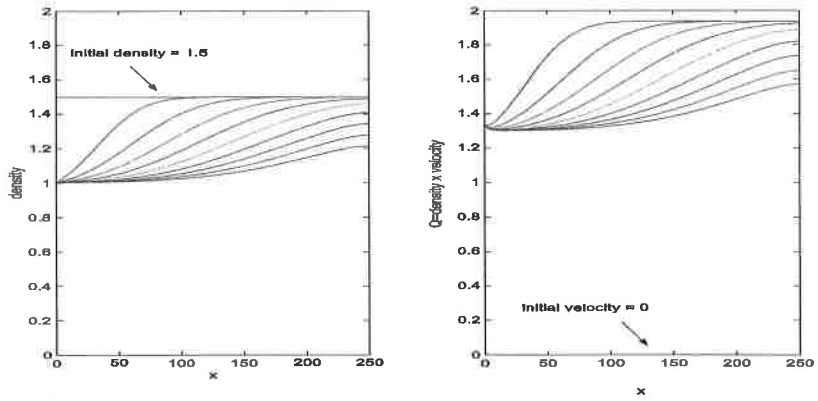

Figure 4.4: Lax-Friedrichs: Constant Initial ($v = 0, \rho = 1.5$) and Boundary Conditions ($\rho(0) = 1, Q(0) = 1.34$)

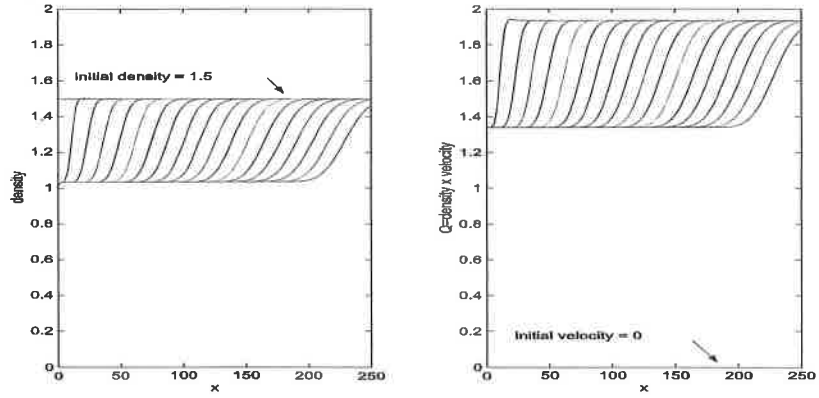

Figure 4.5: Upwind: Constant Initial ($v = 0, \rho = 1.5$) and Boundary Conditions ($\rho(0) = 1, Q(0) = 1.34$)

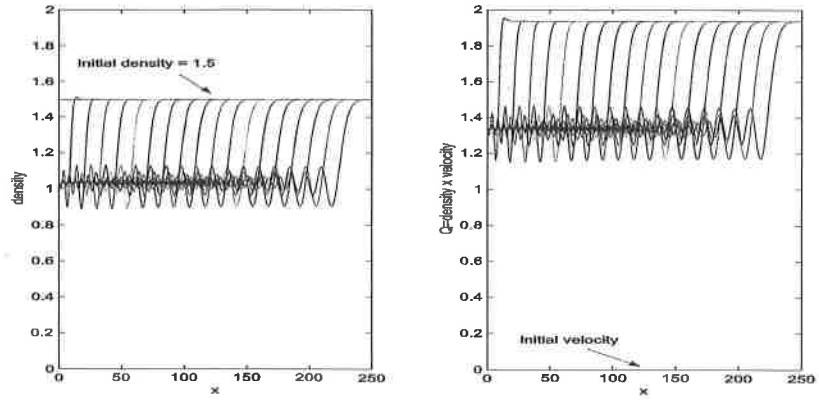

Figure 4.6: Lax Wendroff: Constant Initial ($v = 0, \rho = 1.5$) and Boundary Conditions ($\rho(0) = 1, Q(0) = 1.34$)

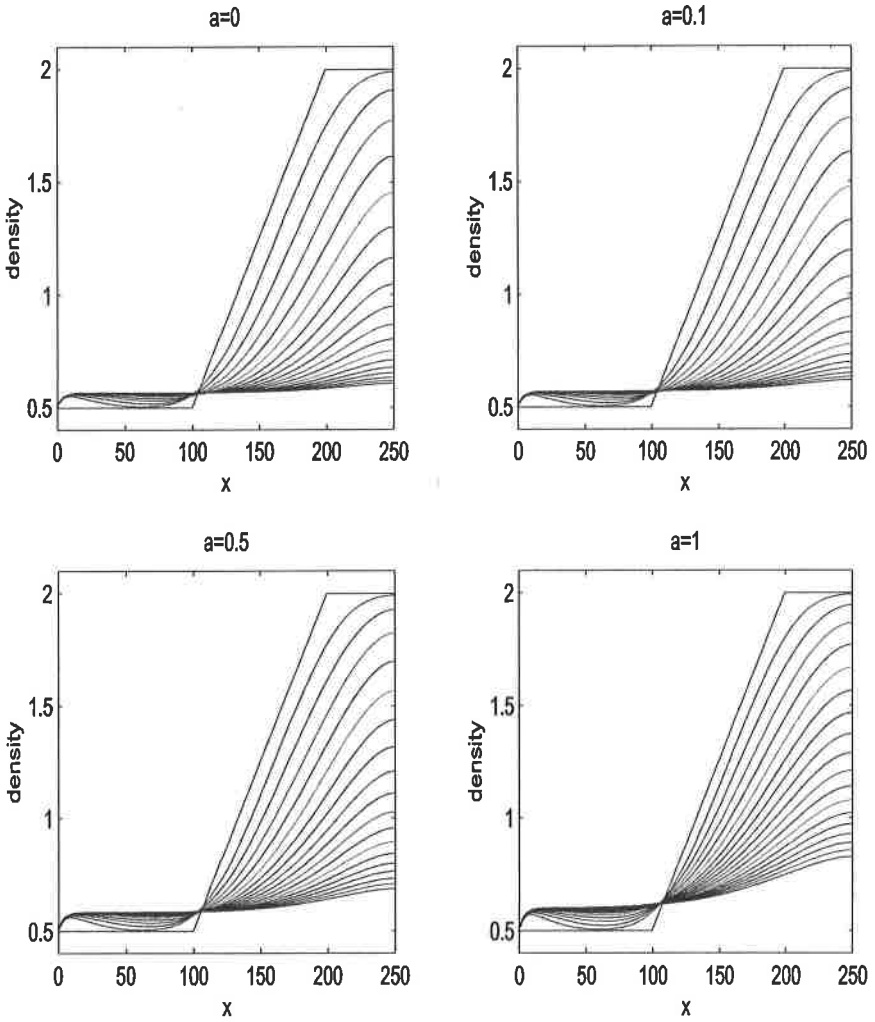

Figure 4.7: Lax-Friedrichs: Varying a with boundary conditions ($\rho(0) = 0.5, Q(0) = 1.1665$)

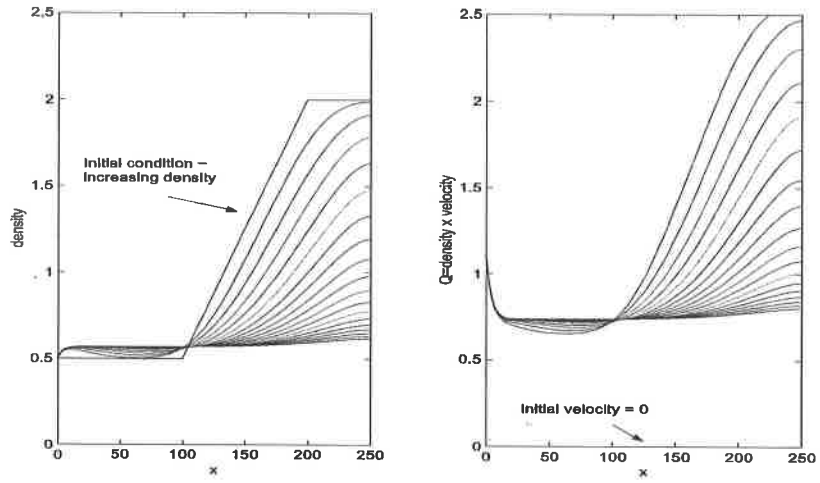

Figure 4.8: Lax-Friedrichs: Increasing Initial and Constant Boundary Condition ($\rho(0) = 0.5, Q(0) = 1.1665$)

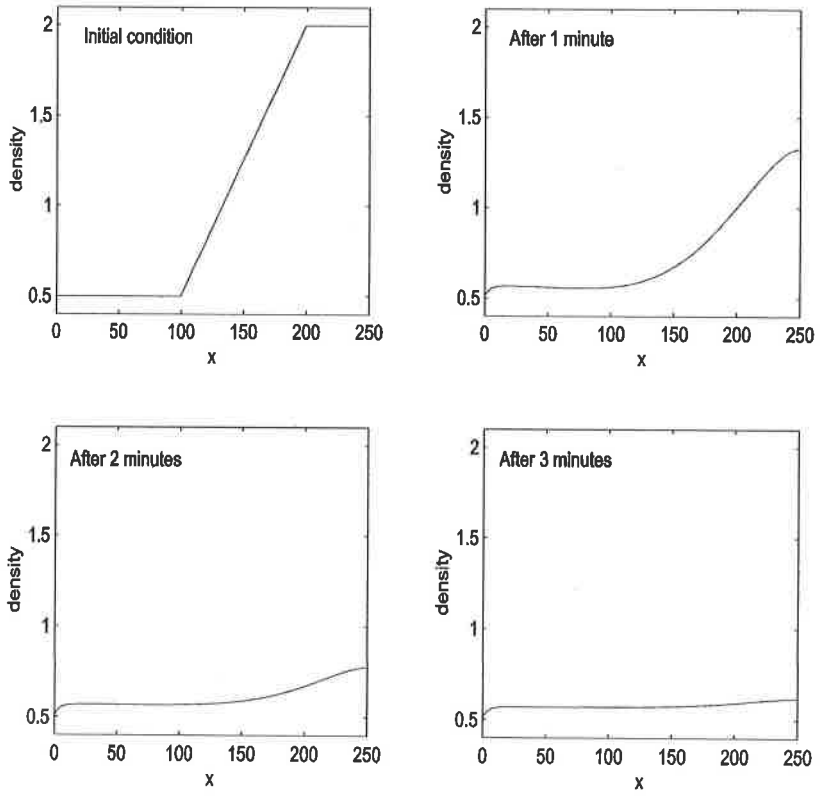

Figure 4.9: Lax-Friedrichs at 1 minute timesteps

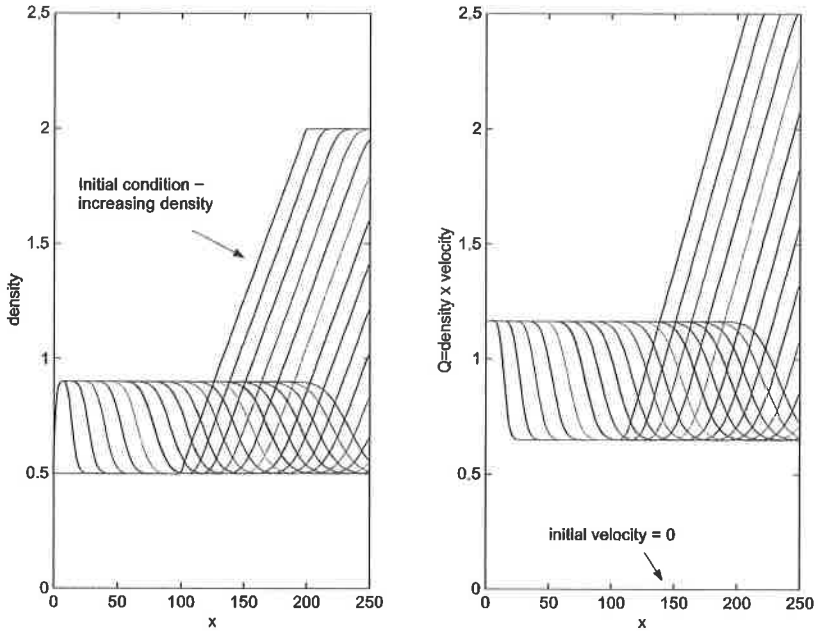

Figure 4.10: Upwind: Increasing Initial and Constant Boundary Conditions ($\rho(0) = 0.5, Q(0) = 1.1665$)

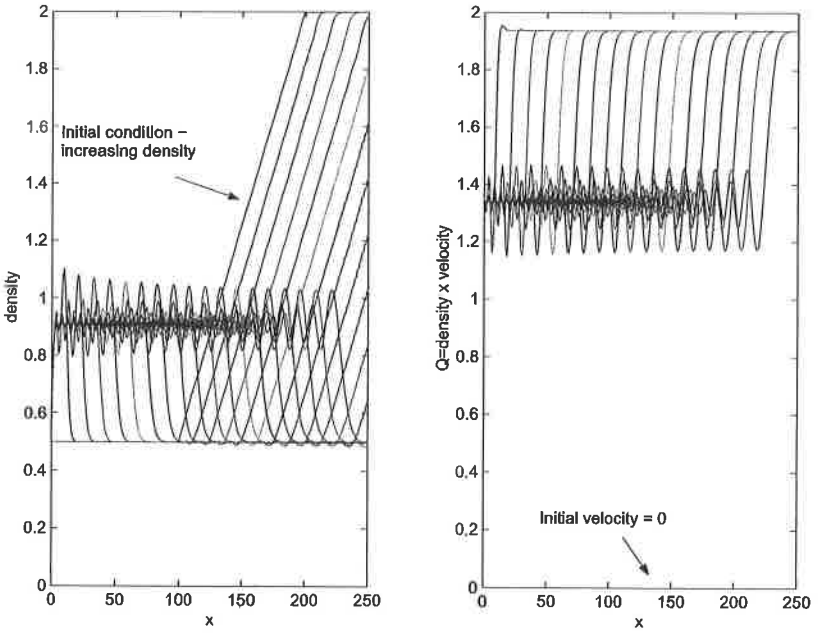

Figure 4.11: Lax-Wendroff: Increasing Initial and Constant Boundary Conditions ($\rho(0) = 0.5, Q(0) = 1.1665$)

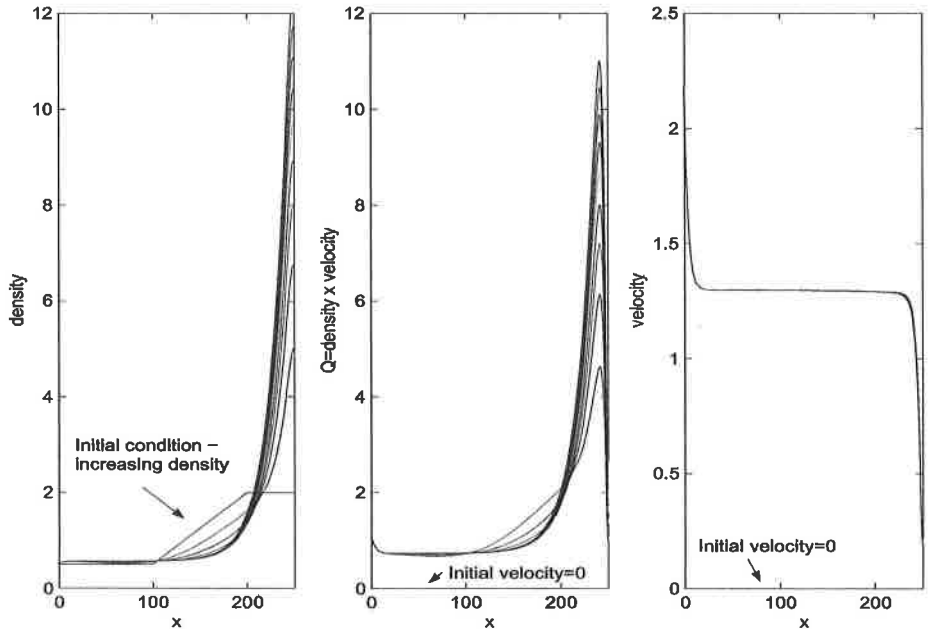

Figure 4.12: Lax-Friedrichs: Increasing Initial and Constant Boundary Conditions ($\rho(0) = 0.5, Q(0) = 1.1665$) but with zero velocity at end

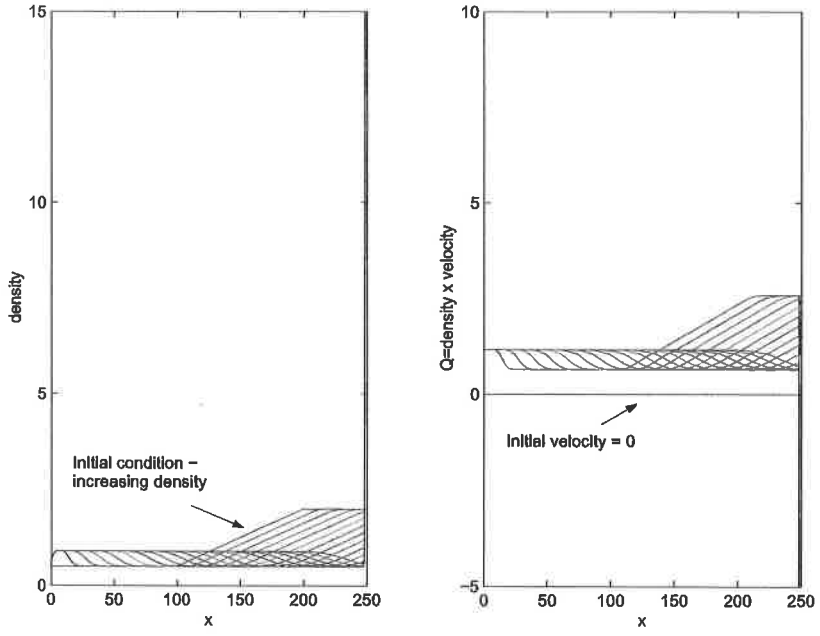

Figure 4.13: Upwind: Increasing Initial and Constant Boundary Conditions ($\rho(0) = 0.5, Q(0) = 1.1665$) but with zero velocity at end

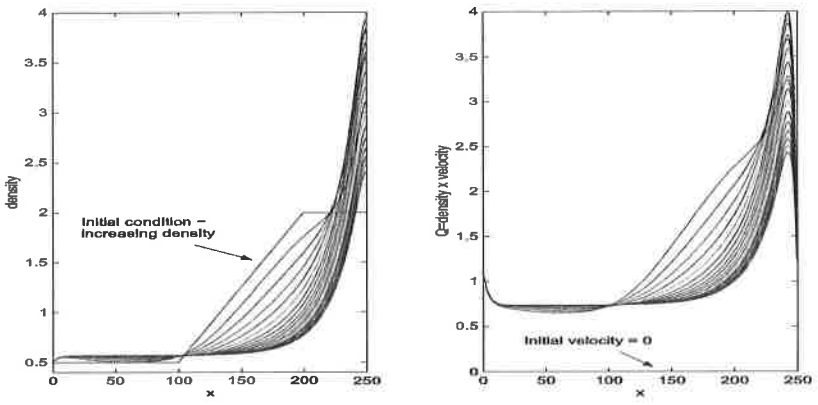

Figure 4.14: Lax-Friedrichs: Increasing Initial and Constant Boundary Conditions ($\rho(0) = 0.5, Q(0) = 1.1665$ but halving velocity at exit)

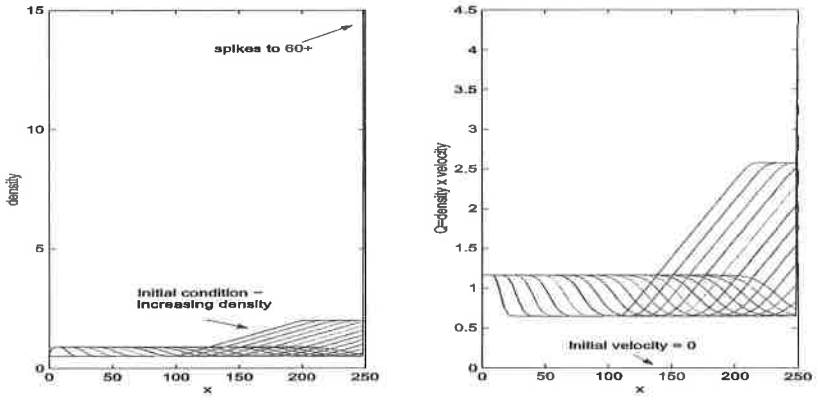

Figure 4.15: Upwind: Increasing Initial and Constant Boundary Conditions ($\rho(0) = 0.5, Q(0) = 1.1665$ but halving velocity at exit)

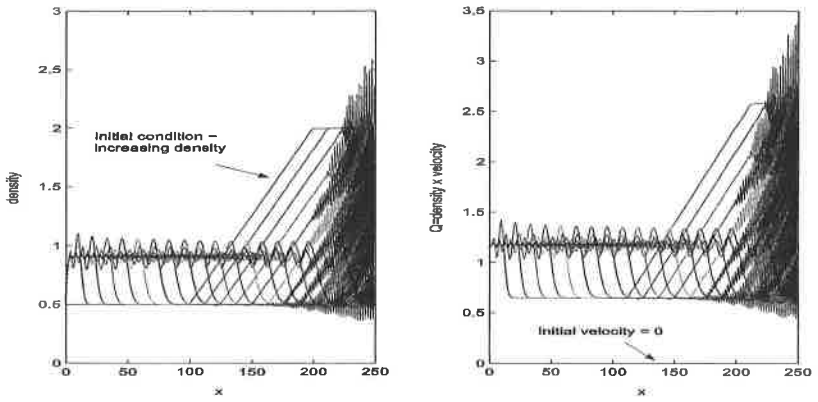

Figure 4.16: Lax-Wendroff: Increasing Initial and Constant Boundary Conditions ($\rho(0) = 0.5, Q(0) = 1.1665$ but halving velocity at exit)

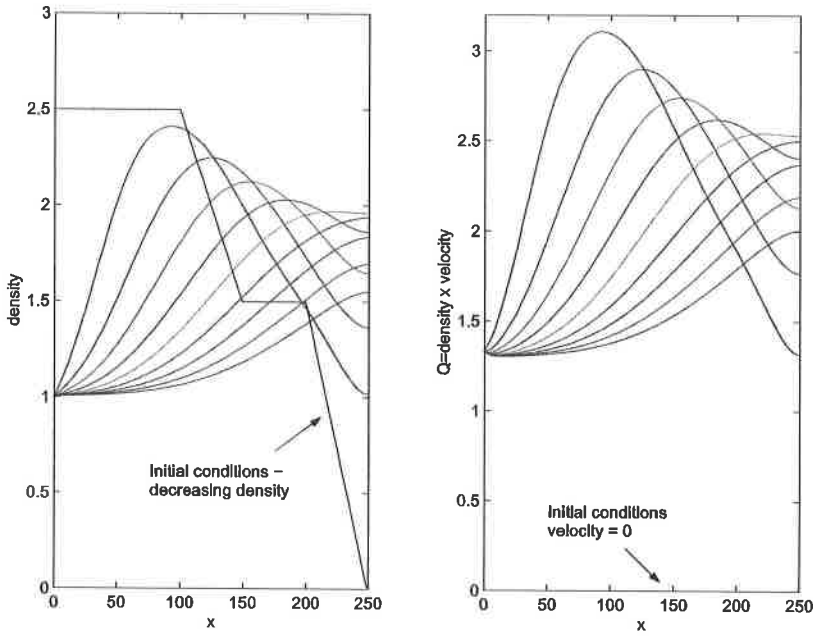

Figure 4.17: Lax-Friedrichs: Decreasing Initial and Constant Boundary Conditions ($\rho(0) = 1.0, Q(0) = 1.34$)

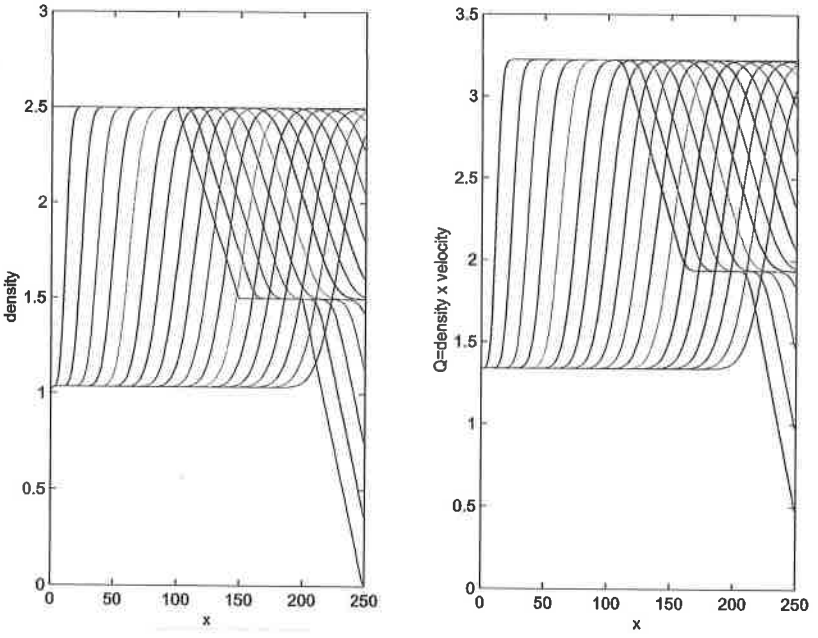

Figure 4.18: Upwind: Decreasing Initial and Constant Boundary Conditions ($\rho(0) = 1.0, Q(0) = 1.34$)

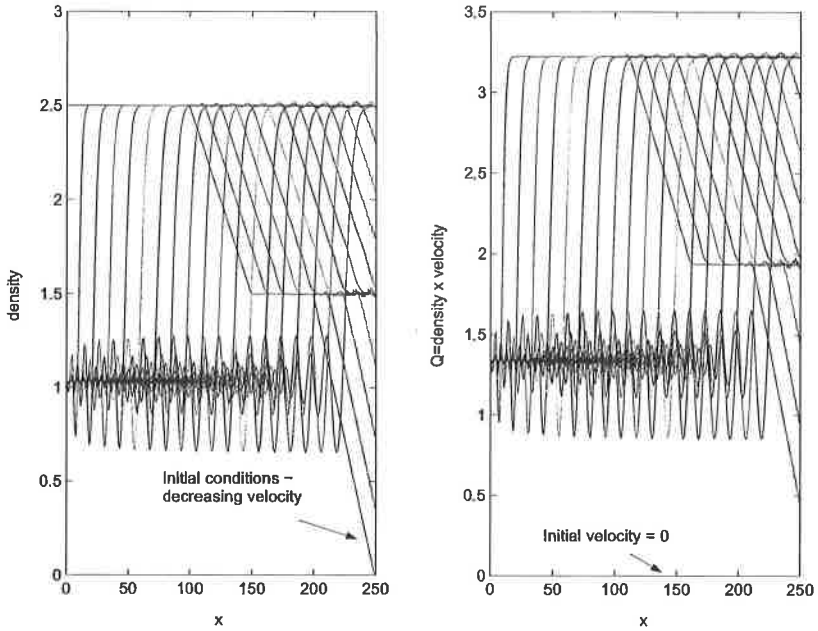

Figure 4.19: Lax Wendroff:Decreasing Initial and Constant Boundary Conditions ($\rho(0) = 1.0, Q(0) = 1.34$)

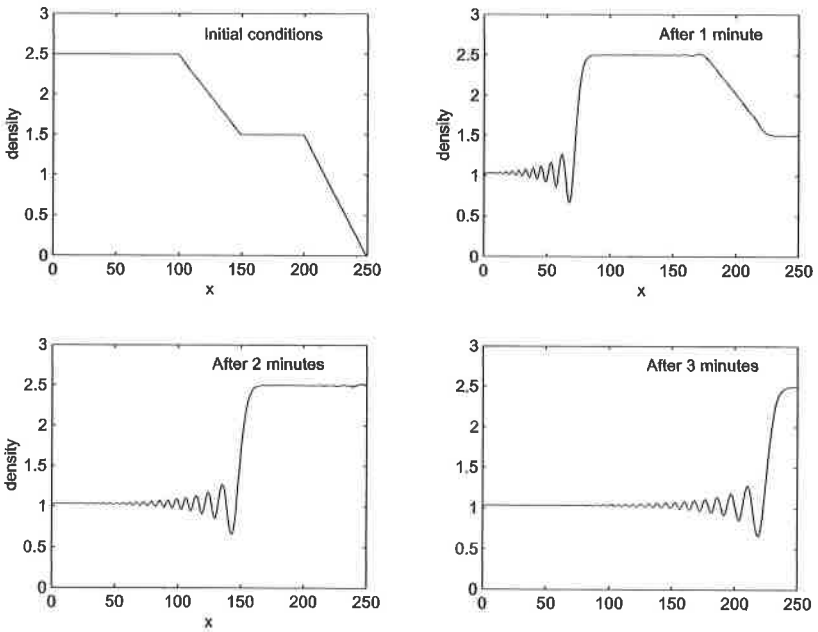

Figure 4.20: Lax Wendroff at 1 minute timesteps

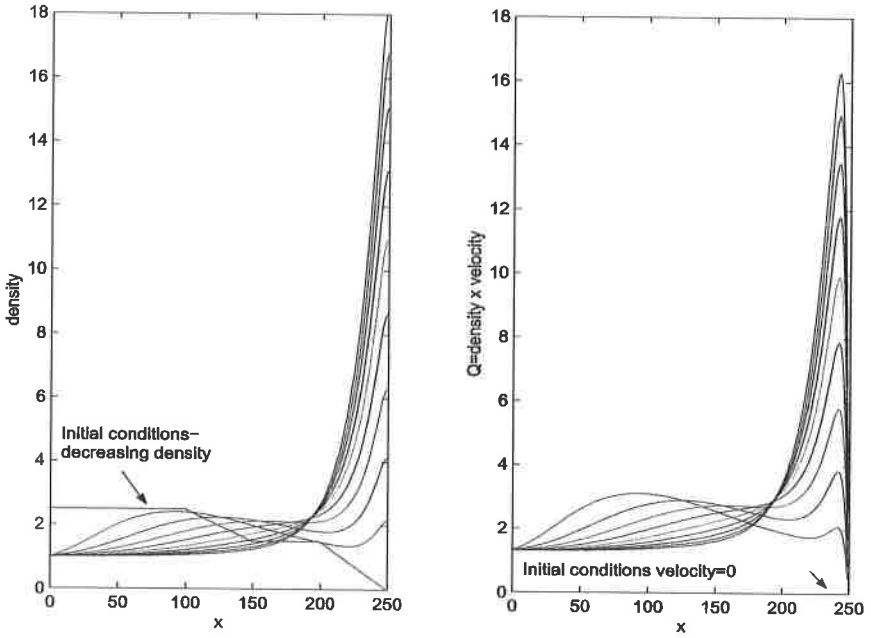

Figure 4.21: Lax-Friedrichs: Decreasing Initial and Constant Boundary Conditions ($\rho(0) = 1.0, Q(0) = 1.34$) but with zero velocity at end

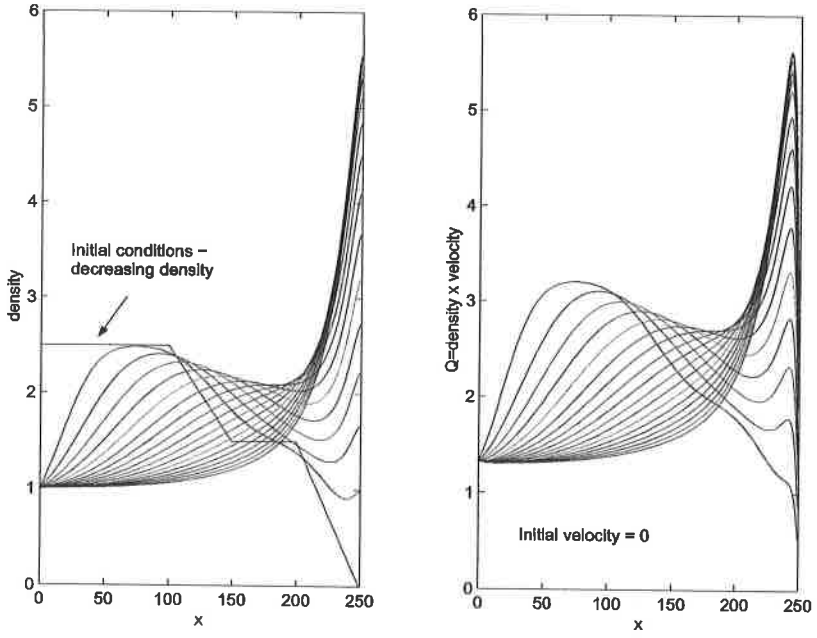

Figure 4.22: Lax-Friedrichs: Decreasing Initial and Constant Boundary Conditions ($\rho(0) = 1.0, Q(0) = 1.34$ but halving velocity at exit)

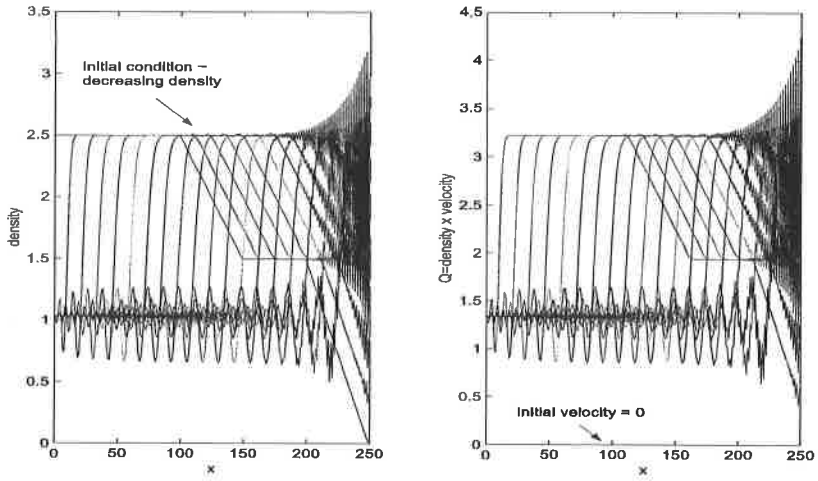

Figure 4.23: Lax Wendroff: Decreasing Initial and Constant Boundary Conditions ($\rho(0) = 1.0, Q(0) = 1.34$ but halving velocity at exit)

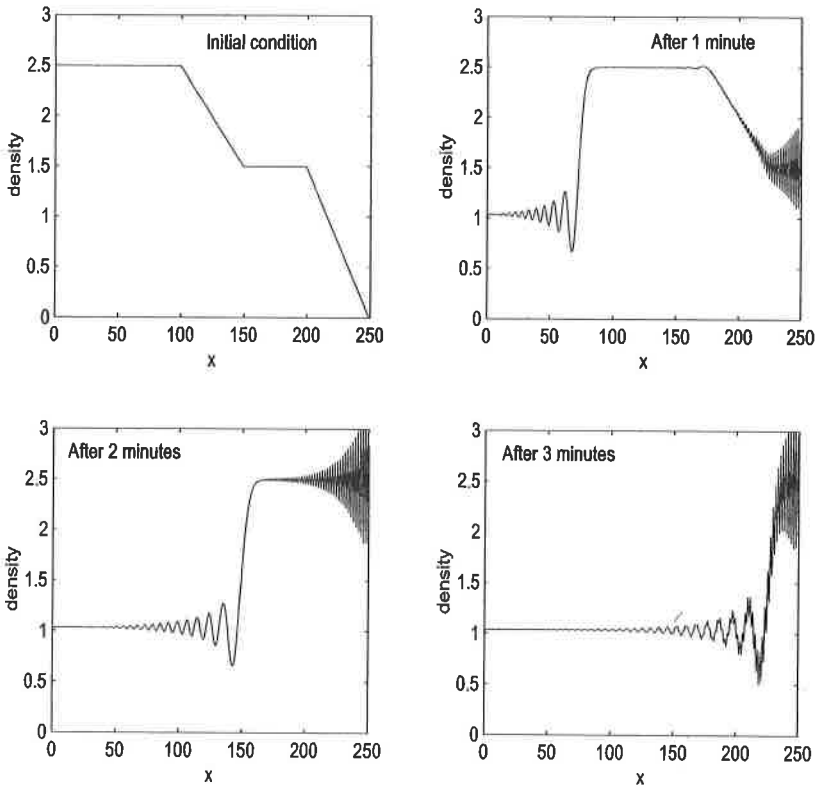

Figure 4.24: Lax-Wendroff in 1 minute timesteps

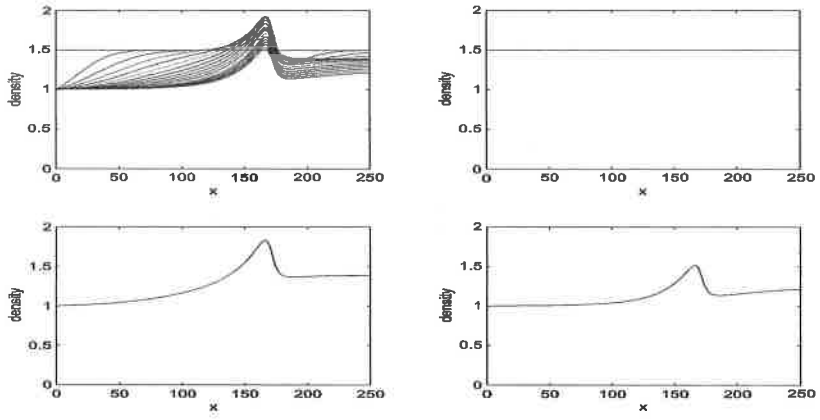

Figure 4.25: Lax-Friedrichs: Constant Initial and Boundary Conditions halving velocity between 170 and 175m)

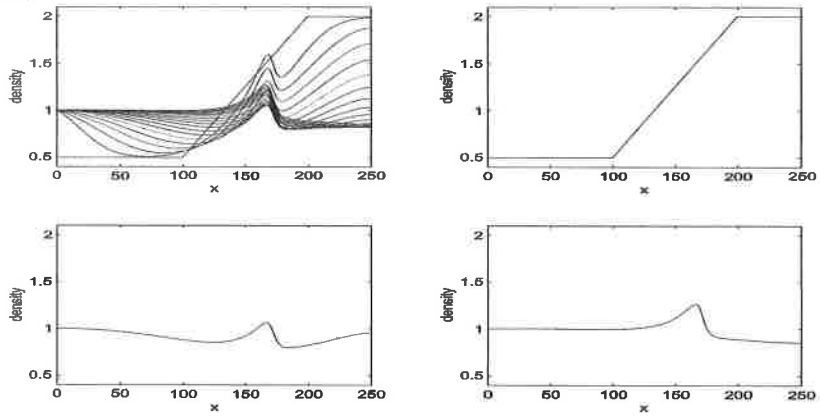

Figure 4.26: Lax-Friedrichs: Increasing Initial and Constant Boundary Conditions halving velocity between 170 and 175m)

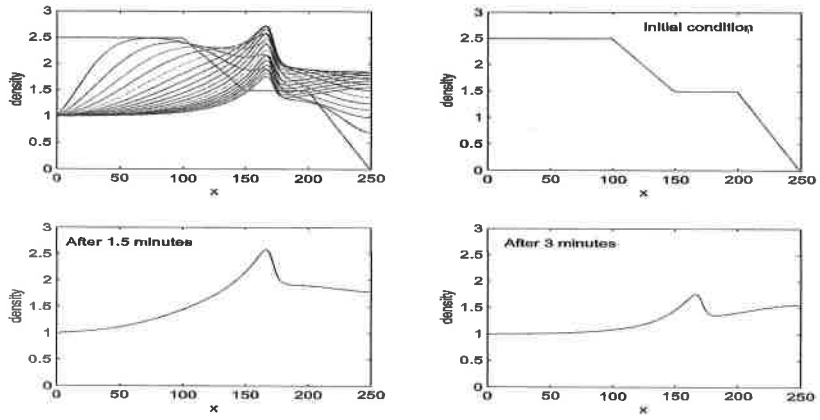

Figure 4.27: Lax-Wendroff: Decreasing Initial and Constant Boundary Conditions halving velocity between 170 and 175m)

Chapter 5

Moving to Two Dimensions

5.1 Introduction

Two dimensional models are much more complicated but far more realistic. Whereas traffic moves naturally in a one lane situation, people will almost always move in an environment which facilitates overtaking, multi-directional and free movement. There would be many different approaches to tackling a 2-D crowd problem. However we will use a similar approach to before and develop a 2-D transformation analogous to Berg's 1-D one and apply it to the Social Force model. Due to time constraints, a simplified numerical scheme is tried where, instead of a full two dimensional scheme, a dimensional splitting approach is used (as outlined in Section 3.6) which treats the x and y components separately; applying say the Lax-Freidrichs scheme first in the x direction alone and then in the y direction alone. Another approach would be to work out x and y values simultaneously on the grid. An example grid is shown overleaf.

5.2 A 2-D Model

As explained above, one way to tackle the two dimensional problem is to calculate an equivalent transformation to the 1-D one of Berg and Woods and substitute it

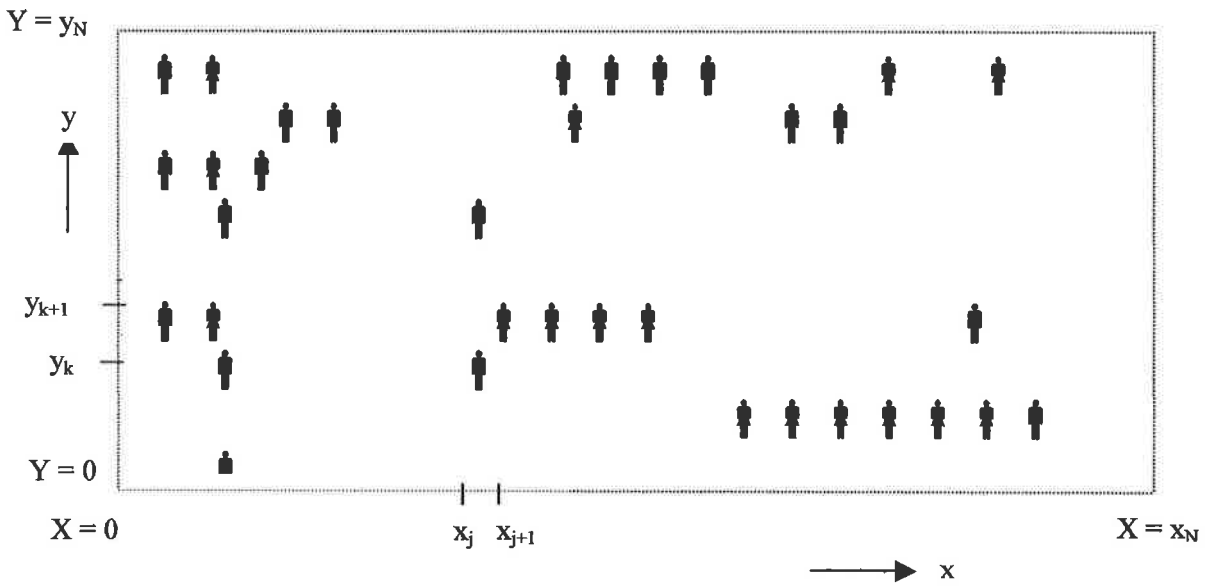

A Two Dimensional Crowd

into the social force model. Following the approach of Berg and Woods, we need an expression for 'headway', b. Working through in a similar way to Section 2.4, we require for a person following model in 2-D that $\int_{y_i}^{y_{i+1}} \int_{x_i}^{x_{i+1}} \rho(x,y,t)dxdy = 1$ and can extend this along and up a corridor of length x_N and width y_N to give

$$\int\int \rho(x+x_N, y+y_N, t)dx_N dy_N.$$

Taking a Taylor expansion in two variables of $\rho(x+x_N, y+y_N, t)$ gives

$$\int\int \Big(\rho(x,y,t) + x_N\rho_x(x,y,t) + y_N\rho_y(x,y,t) + \frac{1}{2!}(x_N^2\rho_{xx}(x,y,t) + 2x_Ny_N\rho_{xy}(x,y,t) +$$

$$y_N^2\rho_{yy}(x,y,t) + \cdots)\Big)dx_N dy_N \tag{5.1}$$

and now we need to integrate over limits appropriate to the 2-D situation. One approach to tackling this is to convert (5.1) into radial coordinates (r,θ) and hence integrate over 0 to 2π for θ and 0 to b for r. Setting $x = rcos\theta$, $y = rsin\theta$ and $r = \sqrt{x^2+y^2}$ we get

$$\int_0^{2\pi}\int_0^b \Big(\rho(r,\theta,t) + r_N cos\theta_N(\rho_r cos\theta - \frac{\rho_\theta sin\theta}{r}) + r_N sin\theta_N(\rho_r sin\theta + \frac{\rho_\theta cos\theta}{r}) +$$

$$\frac{1}{2}(r_N^2 cos^2\theta_N[\frac{\partial\rho_r}{\partial x}\frac{\partial r}{\partial x} + \rho_r\frac{\partial^2 r}{\partial x^2} + \frac{\partial\rho_\theta}{\partial x}\frac{\partial\theta}{\partial x} + \rho_\theta\frac{\partial^2\theta}{\partial x^2}] + 2r_N^2 cos\theta_N sin\theta_N[\frac{\partial\rho_r}{\partial y}\frac{\partial r}{\partial x} + \rho_r\frac{\partial^2 r}{\partial x\partial y} +$$

$$\frac{\partial \rho_\theta}{\partial y}\frac{\partial \theta}{\partial x} + \rho_\theta \frac{\partial^2 \theta}{\partial x \partial y}] + r_N^2 sin^2\theta_N [\frac{\partial \rho_r}{\partial y}\frac{\partial r}{\partial y} + \rho_r \frac{\partial^2 r}{\partial y^2} + \frac{\partial \rho_\theta}{\partial y}\frac{\partial \theta}{\partial y} + \rho_\theta \frac{\partial^2 \theta}{\partial y^2}])\Big) r_N dr_N d\theta_N = 1 \tag{5.2}$$

which, after some algebra, can be expressed as

$$\int_0^{2\pi}\int_0^b \Big(\rho(r,\theta,t) + r_N cos\theta_N(\rho_r cos\theta - \frac{\rho_\theta sin\theta}{r}) + r_N sin\theta_N(\rho_r sin\theta + \frac{\rho_\theta cos\theta}{r}) +$$

$$\frac{1}{2}(r_N^2 cos^2\theta_N[\rho_{rr}cos^2\theta + \frac{\rho_{\theta\theta}sin^2\theta}{r^2} + \frac{2\rho_r sin^2\theta}{r} + \frac{4\rho_\theta sin\theta cos\theta}{r^2}] + 2r_N^2 cos\theta_N sin\theta_N[\rho_{rr}sin\theta cos\theta -$$

$$\frac{2\rho_\theta cos^2\theta}{r^2} + \frac{2\rho_\theta sin^2\theta}{r^2} - \frac{2\rho_r cos\theta sin\theta}{r} - \frac{\rho_{\theta\theta}cos\theta sin\theta}{r^2}] + r_N^2 sin^2\theta_N[\rho_{rr}sin^2\theta + \frac{\rho_{\theta\theta}cos^2\theta}{r^2} +$$

$$\frac{2\rho_r cos^2\theta}{r} - \frac{4\rho_\theta sin\theta cos\theta}{r^2}])\Big) r_N dr_N d\theta_N = 1. \tag{5.3}$$

Integrating with respect to r_N and θ_N results in

$$\Big(\pi b^2\rho + \frac{b^4\pi}{8}(\rho_{rr}cos^2\theta + \frac{\rho_{\theta\theta}sin^2\theta}{r^2} + \frac{2\rho_r sin^2\theta}{r} + \frac{4\rho_\theta sin\theta cos\theta}{r^2}) + \frac{b^4\pi}{8}(\rho_{rr}sin^2\theta +$$

$$\frac{\rho_{\theta\theta}cos^2\theta}{r^2} + \frac{2\rho_r cos^2\theta}{r} - \frac{4\rho_\theta sin\theta cos\theta}{r^2})\Big) = 1 \tag{5.4}$$

which can be simplified to

$$\pi b^2\rho + \frac{b^4\pi}{8}\rho_{rr} + \frac{b^4\pi}{8r^2}\rho_{\theta\theta} + \frac{b^4\pi}{4r} = 1. \tag{5.5}$$

We can solve for b using perturbation analysis by assuming the form $b = A + B\rho_r + C\rho_{\theta\theta} + D\rho_{rr}$, substituting into (5.5) and solving to give

$$b \sim \frac{1}{\sqrt{\pi\rho}} - \frac{\sqrt{\pi\rho}\rho_r}{8r\pi^2\rho^3} - \frac{\sqrt{\pi\rho}\rho_{\theta\theta}}{16r^2\pi^2\rho^3} - \frac{\sqrt{\pi\rho}\rho_{rr}}{16\pi^2\rho^3}. \tag{5.6}$$

Transforming back into x and y coordinates we have

$$b \sim \frac{1}{\sqrt{\pi\rho}} - \frac{\sqrt{\pi\rho}\rho_r}{8r\pi^2\rho^3}(\frac{x\rho_x}{\sqrt{x^2+y^2}} + \frac{y\rho_y}{\sqrt{x^2+y^2}}) - \frac{\sqrt{\pi\rho}\rho_{\theta\theta}}{16r^2\pi^2\rho^3}(y^2\rho_{xx} - y\rho_y - 2xy\rho_{xy} - x\rho_x + x^2\rho_{yy}) -$$

$$\frac{\sqrt{\pi\rho}\rho_{rr}}{16\pi^2\rho^3}(\frac{x^2\rho_{xx}}{x^2+y^2} + \frac{2xy\rho_{xy}}{x^2+y^2} + \frac{y^2\rho_{yy}}{x^2+y^2})$$

$$b \sim \frac{1}{\sqrt{\pi\rho}} - \frac{x\rho_x}{16\rho^{5/2}\pi^{3/2}(x^2+y^2)} - \frac{y\rho_y}{16\rho^{5/2}\pi^{3/2}(x^2+y^2)} - \frac{(\rho_{xx}+\rho_{yy})}{16\pi^{3/2}\rho^{5/2}}. \tag{5.7}$$

Now as before (see Section 4.2) we take d to equal the headway and use Helbing's Behavioural Force Model giving

$$\frac{d\underline{v}_i(t)}{dt} = \frac{\underline{v}_i^0(t)\underline{e}_i^0(t) - \underline{v}_i(t)}{\tau_i} + f(d) \tag{5.8}$$

where $f(d) = A_i exp(\frac{r_{ij}-d_{ij}}{B_{ij}})\underline{n}_{ij}\frac{(1+cos\psi_j)}{2}$, $d \equiv b$ and $\underline{v}$ and $\underline{e}$ are now in vector form. Substituting (5.7) in and expanding in a Taylor series around $\frac{1}{\sqrt{\pi\rho}}$ gives

$$\frac{d\underline{v}_i(t)}{dt} = \frac{\underline{v}_i^0(t)\underline{e}_i^0(t) - \underline{v}_i(t)}{\tau_i} + f(\frac{1}{\sqrt{\pi\rho}}) - (\frac{x\rho_x}{16\rho^{5/2}\pi^{3/2}(x^2+y^2)} - \frac{y\rho_y}{16\rho^{5/2}\pi^{3/2}(x^2+y^2)} -$$

$$-\frac{(\rho_{xx}+\rho_{yy})}{16\pi^{3/2}\rho^{5/2}})f'(\frac{1}{\sqrt{\pi\rho}})). \tag{5.9}$$

As before we can set $f(\frac{1}{\sqrt{\pi\rho}}) = \overline{f}(\sqrt{\pi\rho})$ and $f'(\frac{1}{\sqrt{\pi\rho}}) = -2\sqrt{\pi}\rho^{3/2}\overline{f}'(\sqrt{\pi\rho})$ to give

$$\frac{d\underline{v}}{dt} = \frac{\underline{v}_i^0\underline{e}_i^0 - \underline{v}_i}{\tau_i} + \overline{f}(\sqrt{\pi\rho}) + \overline{f}'(\sqrt{\pi\rho})(\frac{x\rho_x + y\rho_y}{8\rho\pi(x^2+y^2)} + \frac{(\rho_{xx}+\rho_{yy})}{8\pi\rho}). \tag{5.10}$$

Multiplying by ρ, using the conservation law and substituting back for $\overline{f}(\sqrt{\pi\rho})$ and $\overline{f}'(\sqrt{\pi\rho})$ we get a 2-dimensional system of equations

$$\rho_t + (\rho u)_x + (\rho v)_y = 0$$

$$(\rho u)_t + (\rho u^2)_x + (\rho uv)_y = \frac{(u^0e^0 - u)\rho}{\tau} + A\rho exp\Big(\frac{R\sqrt{\pi}\rho^{3/2}-1}{B\sqrt{\pi}\rho}\Big)\underline{n}\frac{1+cos\psi}{2} +$$

$$+(A\underline{n}\frac{1+cos\psi}{2}\frac{R\pi\rho^{3/2}+2\sqrt{\pi}}{2B\pi\rho^2}exp\Big(\frac{R\sqrt{\pi}\rho^{3/2}-1}{B\sqrt{\pi}\rho}\Big)\{\frac{x\rho_x}{8\pi(x^2+y^2)} + \frac{y\rho_y}{8\pi(x^2+y^2)} + \frac{\rho_{xx}+\rho_{yy}}{8\pi\rho}\})$$

$$(\rho v)_t + (\rho uv)_x + (\rho v^2)_y = \frac{(v^0e^0 - v)\rho}{\tau} + A\rho exp\Big(\frac{R\sqrt{\pi}\rho^{3/2}-1}{B\sqrt{\pi}\rho}\Big)\underline{n}\frac{1+cos\psi}{2} +$$

$$+(A\underline{n}\frac{1+cos\psi}{2}\frac{R\pi\rho^{3/2}+2\sqrt{\pi}}{2B\pi\rho^2}exp\Big(\frac{R\sqrt{\pi}\rho^{3/2}-1}{B\sqrt{\pi}\rho}\Big)\{\frac{x\rho_x}{8\pi(x^2+y^2)} + \frac{y\rho_y}{8\pi(x^2+y^2)} + \frac{\rho_{xx}+\rho_{yy}}{8\pi\rho}\}).$$

As an initial approach we are going to numerically solve the above equations by dimensional splitting. As explained before this involves considering only the x direction followed by only the y direction. Therefore we can simplify the model by taking $\underline{n} = -1$ and $\psi = 0 \Rightarrow cos\psi = 1$ for the x-sweep and $\psi = \frac{\pi}{2} \Rightarrow cos\psi = 0$ for

the y-sweep. Letting $\rho u = Q$ and $\rho v = P$, and, as before, splitting the derivative on the right hand side, integrating up and taking over to the left gives:

$$\rho_t + Q_x + P_y = 0$$

$$(Q)_t + \Big(\frac{Q^2}{\rho} + Az\frac{x\rho_x}{8\pi(x^2+y^2)}exp\Big(\frac{R\sqrt{\pi}\rho^{3/2}-1}{B\sqrt{\pi}\rho}\Big)\Big)_x + (\frac{QP}{\rho})_y = \frac{(u^0e^0\rho - Q)}{\tau} -$$

$$-Az\rho exp\Big(\frac{R\sqrt{\pi}\rho^{3/2}-1}{B\sqrt{\pi}\rho}\Big) - \Big(Az\frac{R\pi\rho^{3/2}+2\sqrt{\pi}}{2B\pi\rho^2}exp\Big(\frac{R\sqrt{\pi}\rho^{3/2}-1}{B\sqrt{\pi}\rho}\Big)\{\frac{y\rho_y}{8\pi(x^2+y^2)} + \frac{\rho_{xx}+\rho_{yy}}{8\pi\rho}\}\Big)$$

$$(P)_t + (\frac{QP}{\rho})_x + (\frac{P^2}{\rho} + Az\frac{y\rho_y}{8\pi(x^2+y^2)}exp\Big(\frac{R\sqrt{\pi}\rho^{3/2}-1}{B\sqrt{\pi}\rho}\Big)\Big)_y = \frac{(v^0e^0\rho - P)}{\tau} -$$

$$-Az\rho exp\Big(\frac{R\sqrt{\pi}\rho^{3/2}-1}{B\sqrt{\pi}\rho}\Big) - \Big(Az\frac{R\pi\rho^{3/2}+2\sqrt{\pi}}{2B\pi\rho^2}exp\Big(\frac{R\sqrt{\pi}\rho^{3/2}-1}{B\sqrt{\pi}\rho}\Big)\{\frac{x\rho_x}{8\pi(x^2+y^2)} + \frac{\rho_{xx}+\rho_{yy}}{8\pi\rho}\}\Big)$$

where $z = 1$ for the x-sweep and $z = 0.5$ for the y-sweep.

Stability analysis again requires calculation of the Jacobian matrix, but with a 2-dimensional system [21]

$$\frac{\partial \underline{u}}{\partial t} + \frac{\partial \underline{f}(u)}{\partial x} + \frac{\partial \underline{g}(u)}{\partial y} = 0$$

we have two matrices: $A = \partial \underline{f}/\partial \underline{u}$ and $B = \partial \underline{g}/\partial \underline{u}$. For our system,

$$A = \frac{\partial \underline{f}}{\partial \underline{u}} = \begin{pmatrix} 0 & 1 & 0 \\ \xi_{Q,x} & \frac{2Q}{\rho} & 0 \\ -\frac{Q^2}{\rho^2} & \frac{P}{\rho} & \frac{Q}{\rho} \end{pmatrix}$$

$$B = \frac{\partial \underline{g}}{\partial \underline{u}} = \begin{pmatrix} 0 & 0 & 1 \\ -\frac{Q^2}{\rho^2} & \frac{P}{\rho} & \frac{Q}{\rho} \\ \xi_{P,y} & 0 & \frac{2P}{\rho} \end{pmatrix}$$

where

$$\xi_{S,w} = \frac{-S^2}{\rho^2} + Az(\frac{w}{8\pi(x^2+y^2)})(\frac{R\pi\rho^{3/2}+2\sqrt{\pi}}{2B\pi\rho^2})exp\Big(\frac{R\sqrt{\pi}\rho^{3/2}-1}{B\sqrt{\pi}\rho}\Big).$$

However, calculating stability criteria depends on certain properties of A and B and would require further work.

5.3 Numerics

To solve the system, a dimensional splitting approach using Lax-Friedrichs is adopted. Again we have derivative terms as part of the source term and approximate these as before

$$\rho_x = \frac{\rho^n_{j+1} - \rho^n_{j-1}}{2\triangle x} \qquad \rho_y = \frac{\rho^n_{k+1} - \rho^n_{k-1}}{2\triangle y}$$
$$\rho_{xx} = \frac{\rho^n_{j+1} - 2\rho^n_j + \rho^n_{j-1}}{\triangle x^2} \qquad \rho_{yy} = \frac{\rho^n_{k+1} - 2\rho^n_k + \rho^n_{k-1}}{\triangle y^2}.$$

Using these, and the abbreviations $\zeta = exp\Big(\frac{R\sqrt{\pi}\rho^{3/2}-1}{B\sqrt{\pi}\rho}\Big)$ and $\eta = (\frac{R\pi\rho^{3/2}+2\sqrt{\pi}}{2B\pi\rho^2})$, our scheme becomes

x-sweep

$$\rho^{n+1}_{j,k} = \frac{\rho^n_{j-1,k} + \rho^n_{j+1,k}}{2} - \frac{\triangle t}{2\triangle x}(Q^n_{j+1,k} - Q^n_{j-1,k}) \tag{5.11}$$

$$Q^{n+1}_{j,k} = \frac{Q^n_{j-1,k} + Q^n_{j+1,k}}{2} - \frac{\triangle t}{2\triangle x}\Big([(\frac{Q^2}{\rho})^n_{j+1,k} + A\zeta^n_{j+1,k}(\frac{x(j)}{8\pi(x(j)^2 + y(k)^2)})]-$$
$$[(\frac{Q^2}{\rho})^n_{j-1,k} + A\zeta^n_{j-1,k}(\frac{x(j)}{8\pi(x(j)^2 + y(k)^2)})]\Big) + \triangle t\Big(- A\rho\zeta^n_{j,k} - A\eta^n_{j,k}\zeta^n_{j,k}(\frac{\rho_{xx}}{8\pi\rho^n_j})\Big)$$

$$P^{n+1}_{j,k} = \frac{P^n_{j-1,k} + P^n_{j+1,k}}{2} - \frac{\triangle t}{2\triangle x}\Big((\frac{QP}{\rho})^n_{j+1,k} - (\frac{QP}{\rho})^n_{j-1,k}\Big) + \triangle t\Big(- A\rho\zeta^n_{j,k} -$$
$$A\eta^n_{j,k}\zeta^n_{j,k}(\frac{\rho_x x(j)}{8\pi(x(j)^2 + y(k)^2)} + \frac{\rho_{xx}}{8\pi\rho^n_j})\Big)$$

y-sweep

$$\rho^{n+1}_{j,k} = \frac{\rho^n_{j,k-1} + \rho^n_{j,k+1}}{2} - \frac{\triangle t}{2\triangle x}(P^n_{j,k+1} - P^n_{j,k-1}) \tag{5.12}$$

$$Q^{n+1}_{j,k} = \frac{Q^n_{j,k-1} + Q^n_{j,k+1}}{2} - \frac{\triangle t}{2\triangle x}\Big((\frac{QP}{\rho})^n_{j,k+1} - (\frac{QP}{\rho})^n_{j,k-1}\Big) + \triangle t\Big(- \frac{A\rho}{2}\zeta^n_{j,k} -$$
$$\frac{A}{2}\eta^n_{j,k}\zeta^n_{j,k}(\frac{\rho_y y(k)}{8\pi(x(j)^2 + y(k)^2)} + \frac{\rho_{yy}}{8\pi\rho^n_j})\Big)$$

$$P^{n+1}_{j,k} = \frac{P^n_{j,k-1} + P^n_{j,k+1}}{2} - \frac{\triangle t}{2\triangle x}\Big([(\frac{P^2}{\rho})^n_{j,k+1} + \frac{A}{2}\zeta^n_{j,k+1}(\frac{y(k)}{8\pi(x(j)^2 + y(k)^2)})]-$$
$$[(\frac{P^2}{\rho})^n_{j,k-1} + \frac{A}{2}\zeta^n_{j,k-1}(\frac{y(k)}{8\pi(x(j)^2 + y(k)^2)})]\Big) + \triangle t\Big(- \frac{A\rho}{2}\zeta^n_{j,k} - \frac{A}{2}\eta^n_{j,k}\zeta^n_{j,k}(\frac{\rho_{yy}}{8\pi\rho^n_j})\Big)$$

where values from the x-sweep are fed into the y-sweep, and the relaxation term is dealt with by the Trapezium rule as before.

5.4 Results

Although the above scheme has been programmed up, time constraints mean that results are very preliminary at this stage. Significant further work needs to be undertaken on boundary conditions and stability criteria. Multi-dimensional hyperbolic schemes can cause difficulties at the boundaries. The results shown are based on initial data

$$\rho(x, y) = 1 \qquad \text{at time zero}$$

and left hand boundary conditions

$$\rho(0, y) = \begin{cases} 2.0 & \text{if } y \leq 3 \\ 0.5 & \text{if } y \geq 3 \end{cases}$$

representing a large flow of people into the corridor from one corner and fewer along the rest of the boundary. At other boundaries, ghost points are identified equal to the boundary value except for $P(x, -1) = -P(x, 0)$ and $P(x, y_N + 1) = -P(x, y_N)$ as an attempt to simulate the walls of a corridor. Figures 5.1 to 5.2 show some initial results, with a constant initial density changing, after a period of time, the distribution of people within the corridor created. Figure 5.1 shows the distribution of density in a corridor of length 50 metres and width 10 metres running for 2 seconds, whereas Figure 5.2 shows a corridor of 100 metres (broken into 5 metre spatial steps) with width 10 metres after 10 seconds. Despite the non-smoothness of the graphs, they do appear to exhibit some expected behaviour. This is easier to observe in Figure 5.2 where the high density at one corner feeding into the corridor fans out: we would expect people coming into a corridor at high density to spread out into the space available. It also shows a slight speeding up and bunching effect towards the far end where people catch up others to create a high density but then are able to overtake or spread out to reduce density before catching up the next slow moving group. Computational problems currently arise at the origin or in areas of zero

density, resulting in floating point errors, and also if the program is run for long time periods.

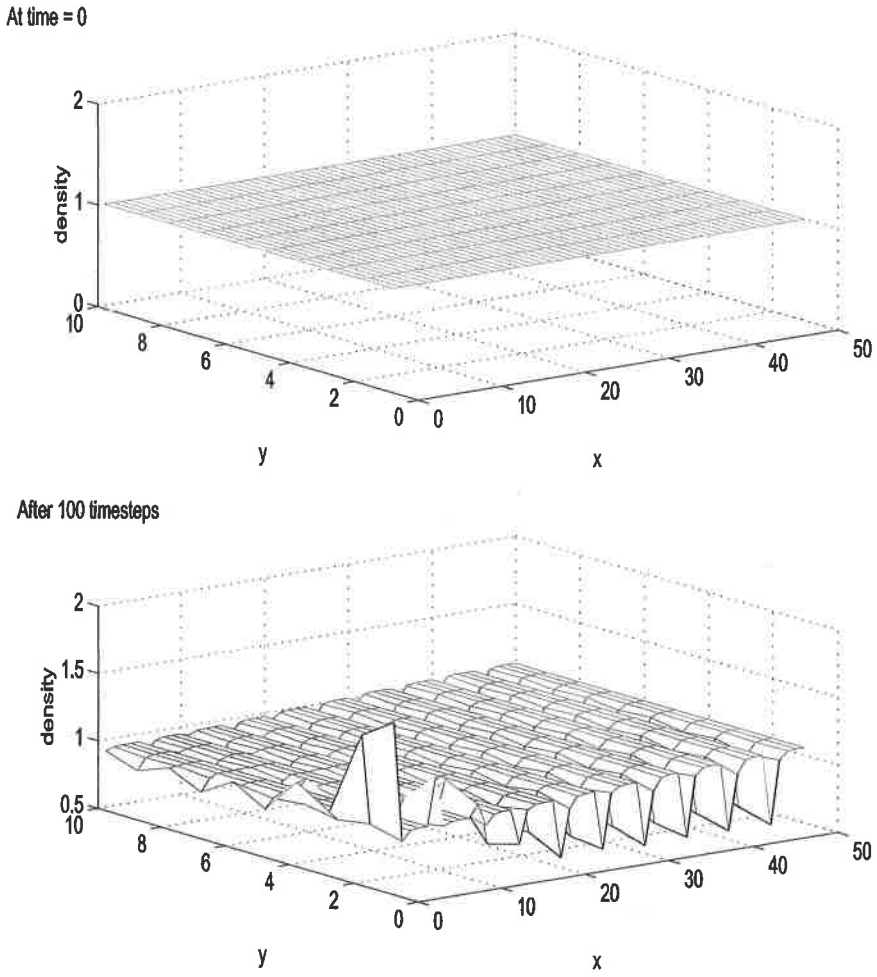

Figure 5.1: Dimensional Stepping - 50m x 10m corridor, $\triangle x = 1, \triangle y = 1, \triangle t = 0.02$

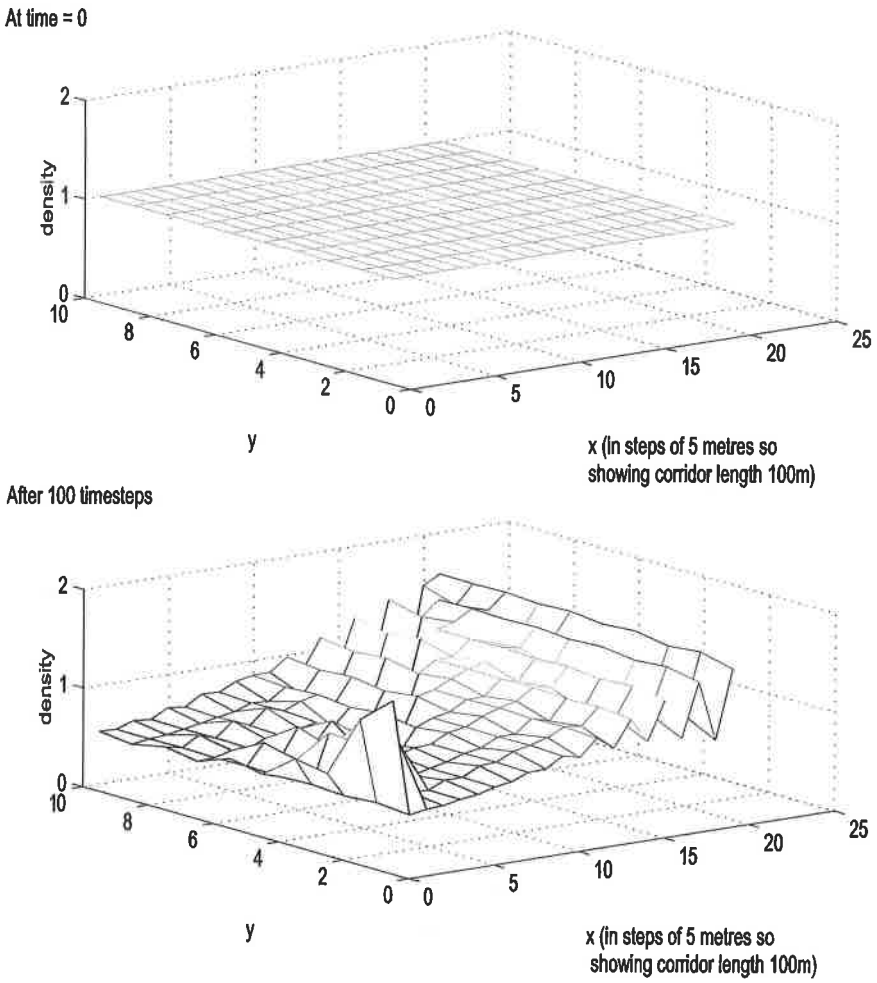

Figure 5.2: Dimensional Stepping - a longer time run, $\triangle x = 5, \triangle y = 1, \triangle t = 0.1$

Chapter 6

Conclusions and Further Research

The aim of this dissertation has been to use a transformation developed by Berg and Woods in a traffic context to move from a microscopic to a macroscopic model of pedestrian dynamics and then to solve this model numerically. It applies the techniques of numerical analysis to a modelling problem linking the psychological behaviour of humans with the rigor of mathematics, drawing heavily on Helbing's Behavioural Force Model. The majority of the work focuses on a 1-dimensional model and excludes physical interactions with other pedestrians and hence is very much a first step.

In 1-D, the transformation is applied to give a system of equations which model movement in one direction in a corridor like scenario. The nature of the model highlighted some interesting numerical problems, with a complicated source term and a stiff relaxation term. Applying the three numerical schemes (Lax-Friedrichs, Upwind and Lax Wendroff) to the model showed that

- for normal movement Upwind gives the most robust results whilst Lax-Friedrichs suffers from diffusion and Lax-Wendroff, although giving a sharp profile, suffers from trailing edge oscillation
- when attempting to model a sudden pile up situation at one end, Lax-Friedrichs

gives results which most closely mirror what we would physically expect

- modelling a gradual pile-up by halving velocity at one end gives physically reasonable results when using Lax-Friedrichs but interesting bifurcation with Lax-Wendroff. This latter behaviour deserves further exploration.

Of course, modelling crowds in 1-D is not physically realistic but it does highlight some of the challenges with this approach, for example trying to force numerical schemes into quasi-physical behaviour, particularly at the boundary, leads to difficulties. However it can be difficult to interpret results if the model is too simplified, although there is scope for developing the 1-D approach further both in terms of the model and numerically:

- including terms for panic and pedestrians bumping into each other
- lifting the assumption that interactions are isotrophic to allow some influence from those behind
- varying constant values and further work into more accurate values
- extending the schemes used for numerically solving the model
- alternative approaches to dealing with the source term and the relaxation term.

However all these will be limited by the 1-D view. Moving into 2-D, interactions with other pedestrians, multi-directional movement and avoidance and attraction components all became relevant and need to be developed. The 2-D work undertaken in chapter 5 merely scratches the surface of a huge topic but does show that a 2-D transformation can be developed and a model deduced from this. It would be beneficial to use the 2-D transformation constructed here in a traffic situation for which there is real life data to test its effectiveness. The model is fairly robust but further work needs to be done on developing the numerics to solve it. Additional

anaylsis needs to be undertaken on stability and setting up boundary conditions to ensure that the problem remains well-posed.

We set out to develop a robust and fairly simple macroscopic model: our model is not that simple but is computationally efficient. Comparisions with other models and assessment for legitimate crowd behaviour is needed to evaluate whether this approach is an improvement on others. There is much scope for further development.

Bibliography

[1] M.Bando, Y.Sugiyama et al *Dynamical model of traffic congestion and numerical simulation* Physical Review E Vol. 51(2) Feb 1995

[2] P.Berg & A.Woods *Relating Car-Following and Continuum Models of Road Traffic* University of Bristol 2000

[3] P.Berg, A.Mason & A.Woods *Continuum Approach to Car-Following Models* Physical Review E Vol. 61(2) Feb 2000

[4] Geoff Bicknell *Case Studies in Advanced Computation Lecture Notes* Research School of Astronomy and Astrophysics, Mt Stromlo Observatory, Australian National University

[5] J.Fruin *Pedestrian and Planning Design* Metropolitan Association of Urban Designers and Environmental Planners 1971

[6] D.Helbing, I.Farkas, P.Molnár & T.Vicsek *Simulation of Pedestrian Crowds in Normal and Evacuation Situations* 2002 pg 21-58 in M.Schreckenberg & SD Sharma (eds) Pedestrian and Evacuation Dynamics (Springer, Berlin)

[7] D.Helbing *A Fluid Dynamic Model for the Movement of Pedestrians* May 1998

[8] D.Helbing & T.Viscek *Optimal Self-organization* New J. Physics I Sept 1999

[9] D.Helbing & P.Molnár *Social Force Model for Pedestrian Dynamics* Physical Review E Vol. 51(5) May 1995

[10] D.Helbing *Traffic and Related Self-Driven Many-Particle Systems* April 2001 (www.helbing.org)

[11] D.Helbing, I.Farkas & T.Viscek *Simulating Dynamical Features of Escape Panic* Nature Vol. 407 28 Sept 2000

[12] D.Helbing, I.Farkas & T. Viscek *Freezing by Heating in a Driven Mesocopic System* Physical Review Letters Vol. 84(6) 7th Feb 2000

[13] D.Helbing *From Microscopic to Macroscopic Traffic Models* June 1998 (www.helbing.org)

[14] D.Helbing & B.Tilch *Generalized Force Model of Traffic Dynamics* Physical Review E Vol. 58(1) July 1998

[15] L.F.Henderson *On the Fluid Mechanics of Human Crowd Motion* Transpn Rev Vol. 8 1974

[16] L.F.Henderson *The Statistics of Crowd Fluids* Nature Vol. 229 5 Feb 1971

[17] J.Hudson *Numerical Techniques for Conservation Laws with Source Terms* MSc Dissertation University of Reading 1998

[18] M.J.Lighthill & G.B.Witham *On Kinematic Waves II. A Theory of Traffic Flow on Long Crowded Roads* Proc. R. Soc. London Ser. A 229 (1955)

[19] D.J. Low *Following the Crowd* Nature Vol. 407 28 Sept 2000

[20] A.D. Mason & A.Woods *Car-following Model of Multispecies Systems of Road Traffic* Physical Review E Vol. 55(3) March 1997

[21] KW Morton & DF Mayers *Numerical Solution of Partial Differential Equations* Cambridge University Press 1994

[22] R.B.Pember *Numerical Methods for Hyperbolic Conservation Laws with Stiff Relaxation 1. Spurious Solutions* SIAM J.Appl Math 53(5) Oct 1993

[23] G.Keith Still *Crowd Dynamics* PhD Thesis University of Warwick 2001

[24] Y.Suzuki & Y-h.Taguchi *New Phases in Optimal Velocity Model* Cooperative Transportation Dynamics 2002

[25] R.J.LeVeque & H.C.Yee *A Study of Numerical Methods for Hyperbolic Conservation Laws with Stiff Source Terms* J.Comput. Physics 86 1990

[26] R.J.LeVeque *Numerical Methods for Conservation Laws* Birkhauser-Verlag 1990

[27] Jo White *Modelling Traffic Behaviour on Networks* PhD Thesis University of Salford 1999

[28] Yanenko *The Method of Fractional Steps* Springer New York 1971

[29] H.Yoshida *Construction of higher order symplectic integrators* Physics Letters A 150, (262) 1990

[30] H.M.Zhang *A Non-equilibrium Traffic Model Devoid of Gas-like Behavior* Transpn Res Pt B 36 pp.275-290 2002